U.S. Department of Energy
HelioCon
Heliostat Consortium for
Concentrating Solar-Thermal Power

HELIOCOMM: A Resilient Wireless Heliostats Communication System

Dr. Eirini Eleni Tsiropoulou, Md Sadman Siraj, Aisha B Rahman

conceptional design • components • integration • mass production • heliostat field

Univ of New Mexico RFP 38488-002
HELIOCOMM System Overview

- Dynamic **clustering** of the heliostats based on their topology and networking characteristics
- Identification of the **cluster-head** in each cluster by additionally considering the heliostats' energy availability
- **Entropy-based routing** accounting for the heliostats' energy availability and the network traffic in order to guarantee minimum end-to-end latency constraints
- Joint **maximization of** each heliostat's **energy efficiency** and **minimization of** its **end-to-end latency**
- **Intelligent bandwidth splitting** in the access and backhaul communication links at each clusterhead following the principles of the **Integrated Access and Backhaul (IAB)-based technology**
- Two-stage optimization approach at the access and the backhaul links to determine the **optimal transmission power of each heliostat** to **achieve** its Quality of Service (QoS) prerequisites, as defined by the **Quantified Performance Targets (QPTs)**

Univ of New Mexico RFP 38488-002
HELIOCOMM System Overview

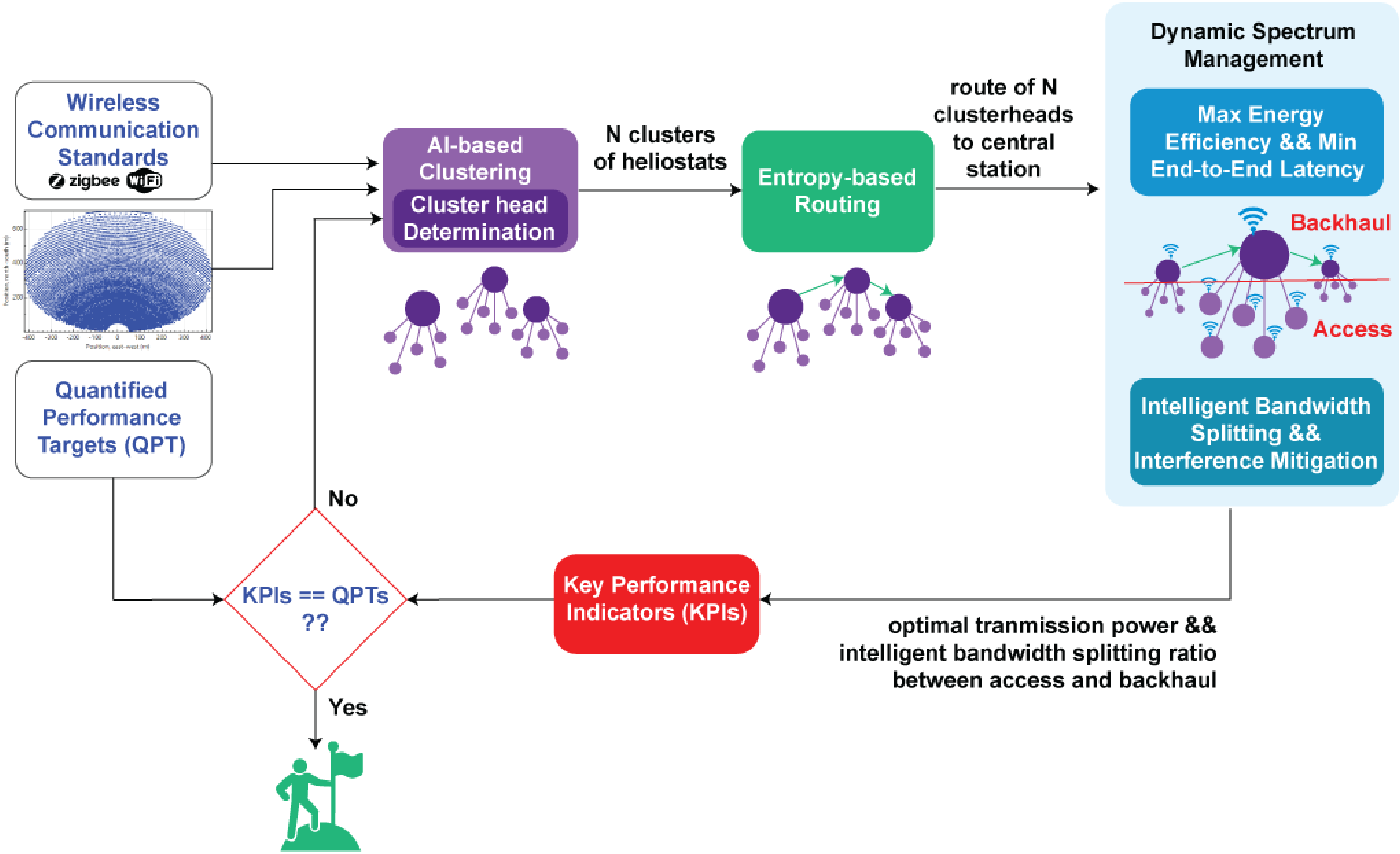

Univ of New Mexico RFP 38488-002
Wireless Communication Standards and QPTs

- HELIOCOMM system tests several wireless communications protocols in different ISM bands
  - 902-928 MHz, e.g., IEEE 802.15.4 (Zigbee, 6LoWPAN)
  - 2400-2483 MHz,
  - 5150-5825 MHz, e.g., IEEE 802.11ax (Wi-Fi 6E)

- Testing in terms of their appropriateness with respect to
  - transmission distance,
  - power consumption,
  - achievable data rates,
  - flexibility of modulation and multiple access techniques

- QPTs are provided as input
  - end-to-end latency,
  - packet error probability,
  - packet losses,
  - energy consumption,
  - transmission power,
  - energy efficiency,
  - network reconfiguration and routing setup time

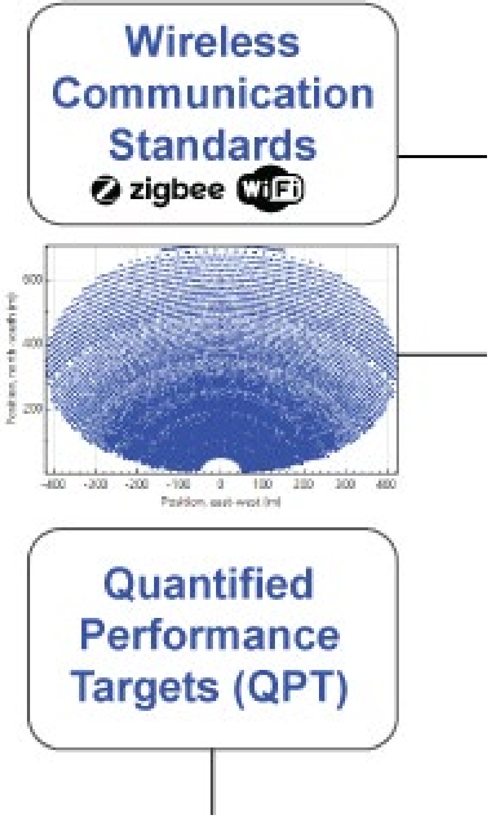

Univ of New Mexico RFP 38488-002
Clustering and Cluster-head Selection

- Artificial intelligent (**AI**) based heliostats **clustering** and cluster-head selection
  - Q-learning-inspired approach
  - Distance and communication channel characteristics (as measured by the Received Signal Strength Indicator – RSSI) are exploited to define the probability of two heliostats belonging in the same cluster.

- Q-learning-inspired algorithm enables each heliostat that acts as a Reinforcement Learning (RL) agent to choose to be connected with another heliostat and form a cluster, i.e., actions

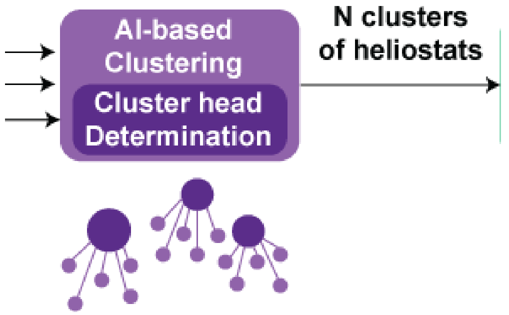

- To balance the RL algorithm's exploration and exploitation processes and improve its computational complexity to converge to a stable clustering in the overall heliostats field, several variations of *ε*-greedy strategies will be tested

- Cluster-head selection for each cluster is performed following the closeness centrality approach and the heliostats' weighted sum of distance and communication channel gain from other heliostats belonging to the same cluster, as well as personal energy availability.

Univ of New Mexico RFP 38488-002
Entropy-based Routing

- Entropy-based routing among the cluster-heads to ultimately forward the information to the central station for further processing to support the autocalibration and closed-loop controls in the heliostats field

- Dynamically determines the optimal routes accounting for the **cluster-heads energy availability and network traffic**

- The cluster-heads act as IAB nodes collecting the information from the heliostats belonging to their own cluster through the access link with a one-hop connection and forwarding in a wireless multi-hop manner in the backhaul link to the central station, i.e., IAB donor.

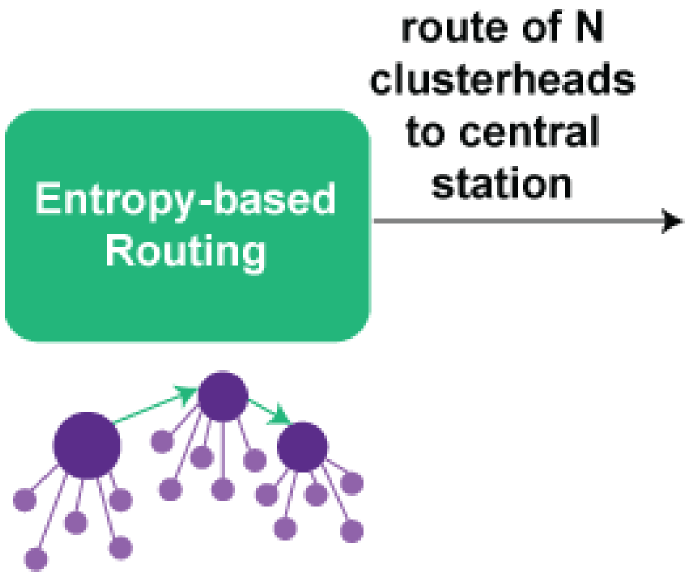

Univ of New Mexico RFP 38488-002
Integrated Access and Backhaul Technology

- Two-stage optimization problem is solved at each IAB node to determine:
  - optimal transmission power
  - intelligent bandwidth splitting in the access and backhaul links
  - **Goal**: joint *maximization of the energy efficiency* and *minimization of the end-to-end latency* experienced by all heliostats in its cluster

- The two-stage optimization problem is split between the access and the backhaul in order to ultimately optimize the experienced energy efficiency of each cluster-heliostat, i.e., cluster-node

- Towards minimizing the end-to-end latency experienced in each route, information about the transmission power levels and the bandwidth splitting in the access and backhaul links should be exchanged among the IAB nodes belonging to the same route

- The multiple two-stage distributed optimization problems within each route are solved in parallel and information is exchanged among the IAB nodes based on beacon signals

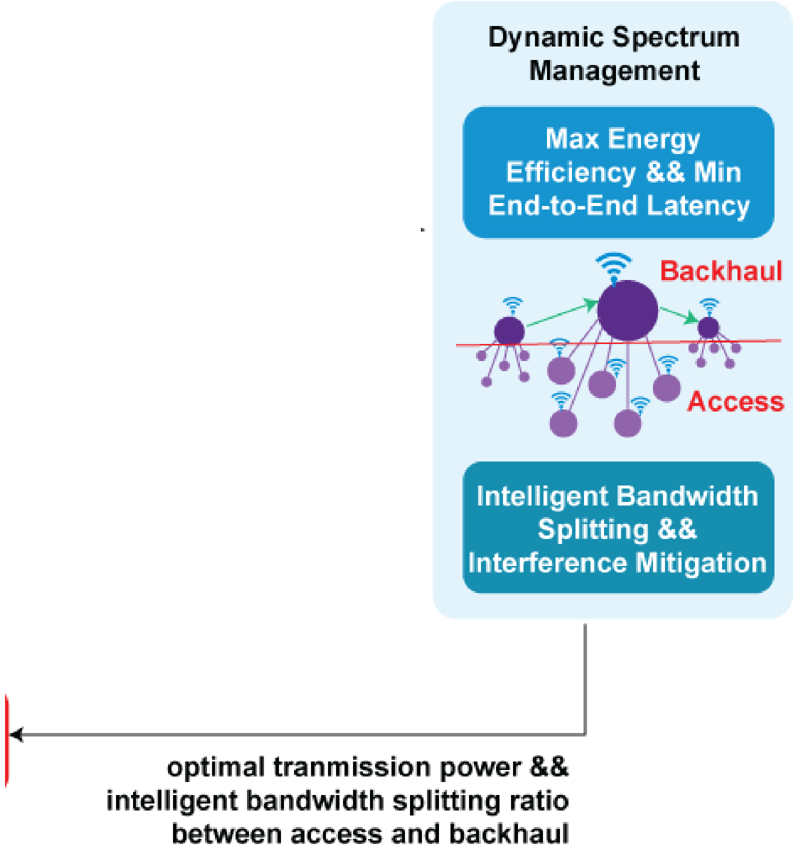

Univ of New Mexico RFP 38488-002
Milestones and Tasks Progress

Design of IAB-based network & optimization of energy efficiency and latency

- Design of a distributed energy efficiency optimization problem satisfying **minimum latency requirements** for access heliostats as well as heliostats operating as IAB nodes in the IAB architecture.
- Two-variable constrained optimization problem in the backhaul level where IAB nodes determine the optimal bandwidth splitting ratio and uplink transmission power.
- Single-variable constrained optimization in the access level for access heliostats to determine the optimal uplink transmission power.
- Collection KPIs for networking metrics based on available wireless communication modules and realistic requirements for wireless heliostats operation:
    - heliostat’s maximum affordable transmission power*,
    - heliostat’s receiver sensitivity*,
    - end-to-end latency constraints considering closed-loop autocalibration and non-closed-loop autocalibration.
- Prepared and submitted a paper to the IEEE IT Professional Magazine presenting the HELIOCOMM System, and to ASME ES, HelioCon 2024 workshop presenting our initial communication latency findings.

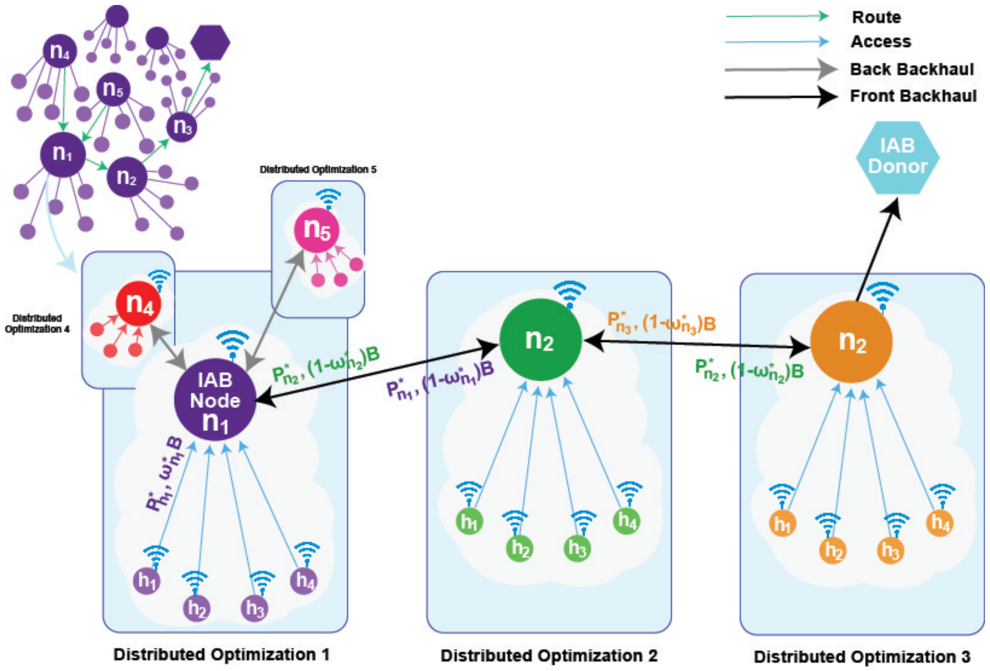

*based on the technical characteristics of indicative wireless modules TI CC1312R and TI CC1352R

Univ of New Mexico RFP 38488-002
Milestones and Tasks Progress

Testing of IEEE 802.11ax and IEEE 802.15.4 under the IAB-based network

- Characteristics of the standards IEEE 802.11ax and IEEE 802.15.4 are employed during the simulation of the IAB network in the CSP field.

- Under the standards, the optimization problem is solved in order to analyze the resulting KPI values.

zigbee OR Wi Fi 6

Dynamic spectrum management in the access and wireless backhaul

- Solving the optimization problem, spectrum is intelligently split and allocated to the access and the backhaul network.
- Based on the allocated spectrum and the uplink transmission power and end-to-end latency constraints, the achieved data rates are derived and analyzed.
- The ultimate goal is to maximize the energy efficiency while satisfying the sub-second end-to-end latency constraints (250 msec) to support closed-loop autocalibration functionalities.
- For the heliostats that do no perform closed-loop autocalibration, the end-to-end latency constraint is more relaxed and currently set to 2 sec.
- Tested the formulated optimization problem in a small-scale heliostat field following the topology of NSTTF@ SNL.

Univ of New Mexico RFP 38488-002
Milestones and Tasks Progress

- NSTTF@SNL Topology
  - Implementation of segmentation in a small-scale heliostat field following the Sandia's NSTTF topology.
  - Access Points (APs) play the role of IAB nodes (APs to be replaced with cluster-heads in the future)
  - Application of Dijkstra's algorithm for the considered APs in the NSTTF topology (Dijkstra's algorithm to be replaced with entropy-based routing in the future).
  - Solving the optimal bandwidth splitting and transmission power problems with the Max. Energy Efficiency && Min. Latency algorithm.
  - Evaluation of the simulation results from the IAB-integrated Max EE && Min Latency wireless communication system.

- Baseline NREL Topology
  - Determination of segment-heads using closeness centrality and energy availability based on the collected energy harvest dataset.
  - Determination of CLA segment groups that can simultaneously perform closed-loop autocalibration while ensuring minimal interference.
  - Solving the optimal bandwidth splitting and transmission power problems with the Max. Energy Efficiency && Min. Latency algorithm.
  - Evaluation of the simulation results from the IAB-integrated Max EE && Min Latency wireless communication system. Simulation was performed for one-day timeframe which included both closed-loop autocalibration and non-closed-loop autocalibration.

NSTTF@SNL

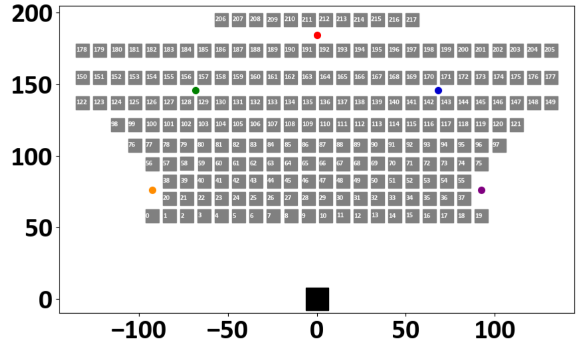

HELIOCON Baseline

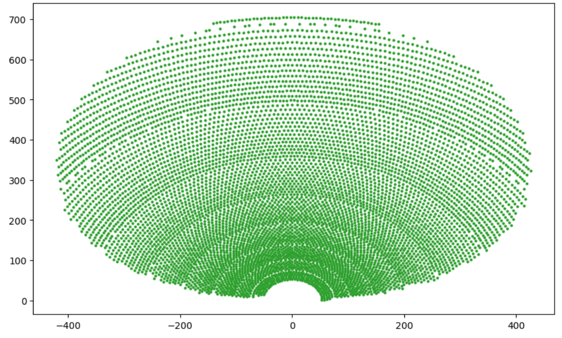

Univ of New Mexico RFP 38488-002
Milestones and Tasks Progress

Emulation-based experiments

- Implementation of the Sandia's NSTTF topology as the test topology with **wired connections** having multiple segments and IAB nodes (can be APs or segment-heads) for **benchmarking** purposes.

- Development of **custom radio and radio medium in OMNET++** to account for the novel IAB network characteristics.

- Integration of the **3GPP wireless path loss** model used in the Python simulations (currently, OMNET++ do not offer 3GPP path loss modeling).

- Establishing the access network with access heliostats and the backhaul network with the IAB nodes in OMNET++ to have the overall IAB architecture.

- **Linking the parameters from Python simulation** such as access data rate, backhaul data rate, access power and IAB node power as input to the OMNET++ experiment.

U.S. Department of Energy
HelioCon
Heliostat Consortium for
Concentrating Solar-Thermal Power

Simulation and Emulation NSTTF@SNL Topology

conceptional design • components • integration • mass production • heliostat field

Energy efficiency optimization for IAB nodes within sub-second latency

- The optimization problem of the IAB nodes is formulated as follows.

$$\max_{\omega_c, P_{N_c}} EE_{N_c}(\omega_c, P_{N_c}) = \frac{R_{N_c}^{BH}}{\sum_{\forall h \in \mathcal{H}_c} P_{h_c} + \sum_{\forall c' \in \mathcal{N}_{N_c}^{\mathcal{BH}}} P_{N_{c'}} + P_{N_c}}$$

$$\begin{aligned} s.t.\ \boldsymbol{c1}&: 0 \leq \omega_c \leq 1 \\ \boldsymbol{c2}&: P_{N_c} \leq P^{max} \\ \boldsymbol{c3}&: P_{N_{c+1}}^{S} \geq P^{s} \\ \boldsymbol{c4}&: t_{h_c}^{E2E} \leq t^{max}, \forall h_c \in \mathcal{H}_c \end{aligned}$$

- The resulting data rate achieved at the backhaul by IAB node N_c is given as:

$$R_{N_c}^{BH} = (1 - \omega_c) B_c \log_2 \left(1 + \frac{g_{N_c} P_{N_c}}{\sum_{\forall i \in \mathcal{I}_{N_c}} g_i P_i + (1 - \omega_c) B_c N_0} \right)$$

Energy efficiency optimization for access heliostats within sub-second latency

- The single-variable optimization problem of the access heliostats is formulated as follows:

$$\max_{P_{h_c}} EE_{h_c}(P_{h_c}, P_{-h_c}) = \frac{R_{h_c}^{AC}}{P_{h_c} + P_c}$$

$$\boldsymbol{c1}: P_{h_c} \leq P^{max}$$

$$\boldsymbol{c2}: P_{h_c,N_c}^{S} \geq P^{s}, \forall h_c \in \mathcal{H}_c$$

$$\boldsymbol{c3}:\ t_{h_c}^{E2E} \leq t^{max}, \forall h_c \in \mathcal{H}_c$$

- The resulting data rate achieved at the access network by heliostat h_c is given as:

$$R_{h_c}^{AC} = \omega_c B_c \log_2\left(1 + \frac{g_{h_c} P_{h_c}}{\sum_{\forall i \in \mathcal{I}_{h_c}} g_i P_i + \omega_c B_c N_0}\right)$$

Univ of New Mexico RFP 38488-002
Energy Efficiency Optimization

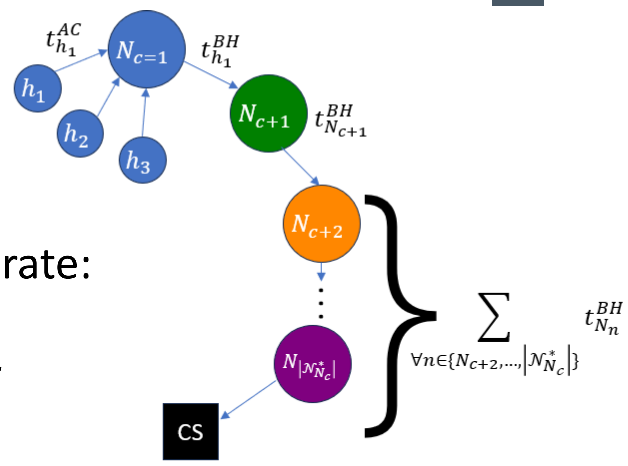

Energy efficiency optimization within sub-second latency

- The corresponding transmission delay experienced by heliostat h_c with the achieved data rate:

$$t^{E2E}_{h_c} = t^{AC}_{h_c} + t^{BH}_{h_c} + t^{BH}_{N_{c+1}} + \sum_{\forall n\in\{N_{c+2},\dots,|\mathcal{N}^*_{N_c}|\}} t^{BH}_{N_n} \le t^{max}, \forall h_c \in \mathcal{H}_c$$

- Where, the delay experienced in the access network and the backhaul network of its own segment is given by

$t^{AC}_{h_c} = \frac{D_{h_c}}{R^{AC}_{h_c}}$ and $t^{BH}_{h_c} = \frac{D_{h_c}}{\frac{R^{AC}_{h_c}}{\sum_{\forall h_c\in\mathcal{H}_c} R^{AC}_{h_c} + \sum_{\forall c'\in\mathcal{N}^{BH}_{N_c}} R^{BH}_{N_{c'}}} R^{BH}_{N_c}}$, respectively.

- The rest of the term $t_{N_{c+1}}$ and $t^{BH}_{N_n}$ capture the latency experienced at the backhaul of the subsequent segment-heads within the route of data transmission from heliostat h_c to the CS, and are given as

$\frac{\sum_{h_c\in\mathcal{H}_c} D_{h_c}}{\frac{R^{BH}_{N_c}}{\sum_{\forall h_{c+1}\in\mathcal{H}_{c+1}} R^{AC}_{h_{c+1}} + \sum_{\forall c'\in\mathcal{N}^{BH}_{\mathcal{N}_{c+1}}} R^{BH}_{N_{c'}}} R^{BH}_{N_{c+1}}}$ and $\frac{D_{N_{n-1}}}{\frac{R^{BH}_{N_{n-1}}}{\sum_{\forall h_n\in\mathcal{H}_n} R^{AC}_{h_n} + \sum_{\forall c'\in\mathcal{N}^{BH}_{\mathcal{N}_n}} R^{BH}_{N_{c'}}} R^{BH}_{N_n}}$, respectively.

Univ of New Mexico RFP 38488-002
Segmentation

Segmentation in NSTFF@SNL topology

- Heliostats are grouped into five segments and each segment is assigned an AP acting as the IAB node (we initiate our experiments with APs, which will be substituted by segment-heads, i.e., heliostats' wireless module).

- The segmentation is however, performed in a simplistic way based on **balancing the number of heliostats per segment and the proximity of the heliostats in a segment to the nearest IAB Node.**

- Based on this segmentation, we determine 5 segments with the following distributions: **Segment 1** – 40, **Segment 2** and **Segment 3** – 43, **Segment 4** and **Segment 5** – 46 heliostats.

- 3GPP path loss model following the [ETSI standard] is used to determine the path loss between a heliostat and its corresponding AP.

- The heliostats are identified with a unique ID based on the channel condition (path loss) between the heliostat and the corresponding IAB Node.

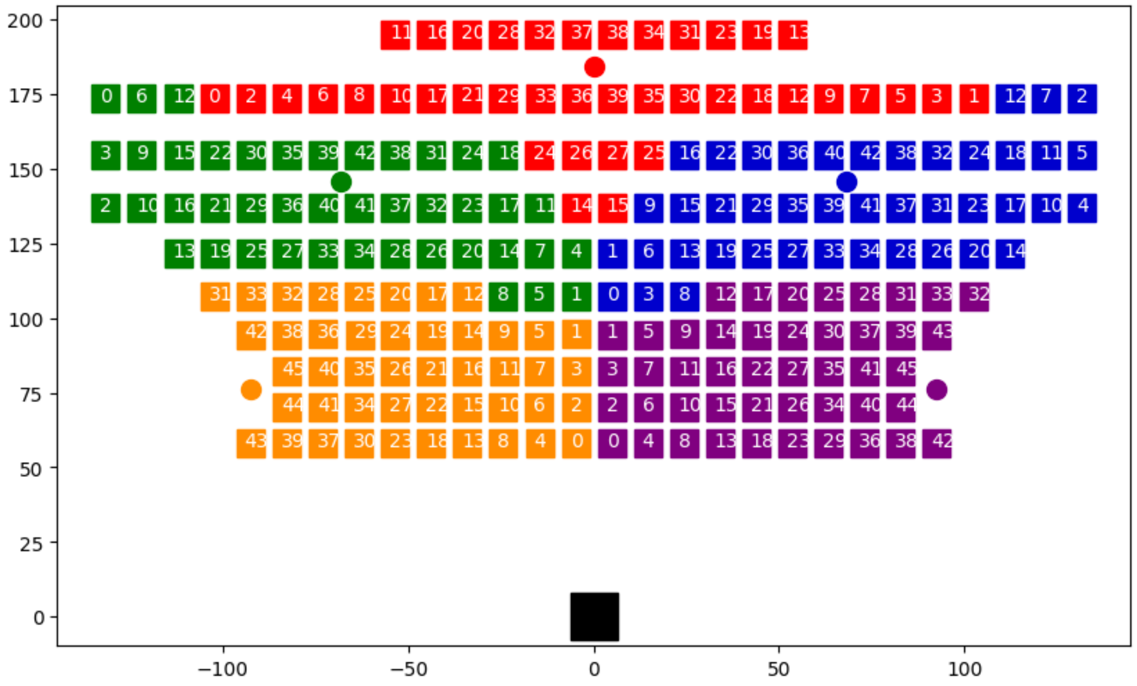

Univ of New Mexico RFP 38488-002
Routing

Routing in NSTFF@SNL topology

- The optimal route is determined following the **Dijkstra's algorithm** (shortest-path algorithm, meaning lowest cost – not necessarily distance).

- The basis of finding the optimal route, considering all the intermediate IAB nodes, is to establish an end-to-end path to the central station with the **lowest total cost**.

- In this application, the **cost** is taken to be **path loss** determined with the 3GPP model and the optimal route is the end-to-end path with the lowest path loss.

- Here, an IAB node can forward the data of its segment to another IAB node and the former IAB node is considered to have a backhaul connection to the latter IAB node.

- Each IAB node is required to allocate its backhaul bandwidth to its associated heliostats as well as to the IAB node(s) connected to its backhaul.

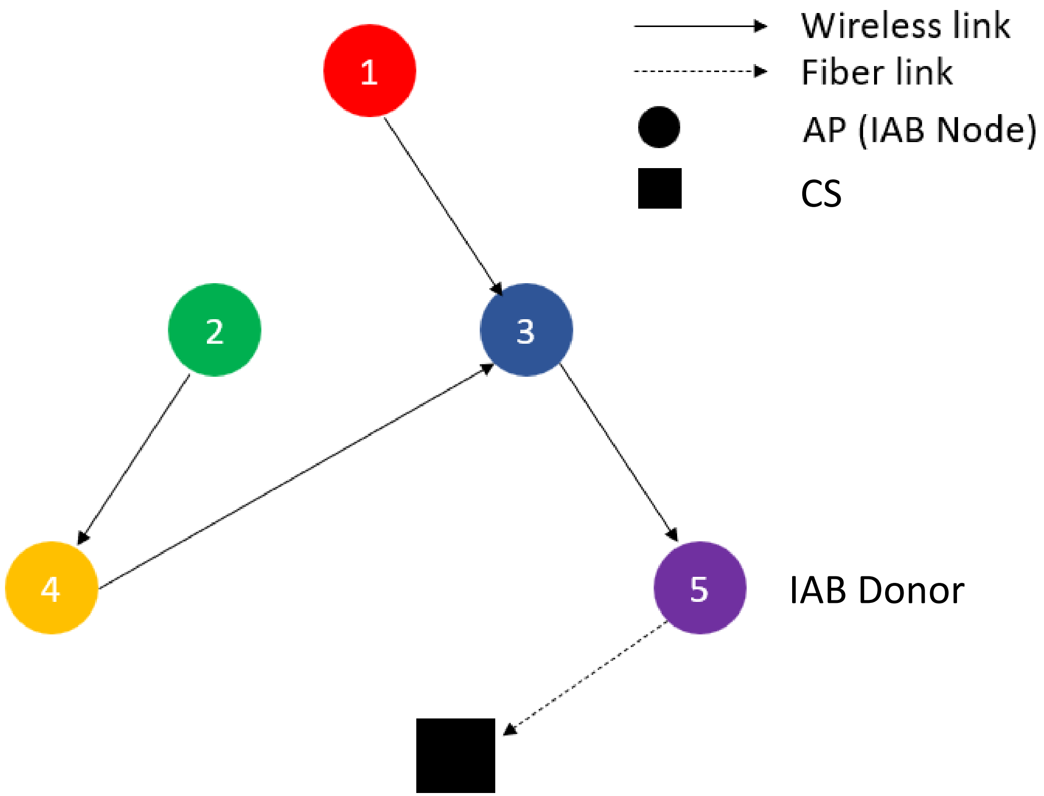

Simulation Results

Transmission Power

- Considering the transmission power bound of the modules TI CC1312R and TI CC1352R, the maximum transmission power is set to 25mW.
- The **higher the ID of a heliostat** in a segment, the **higher** is its **channel gain** with the IAB node. This results in a **lower transmission power** required for a heliostat with higher IDs.
- Due to interference among the simultaneously transmitting heliostats connected to the same AP, **the more the number of heliostats in a segment, the higher the interference, hence, the heliostats transmit with higher power.**

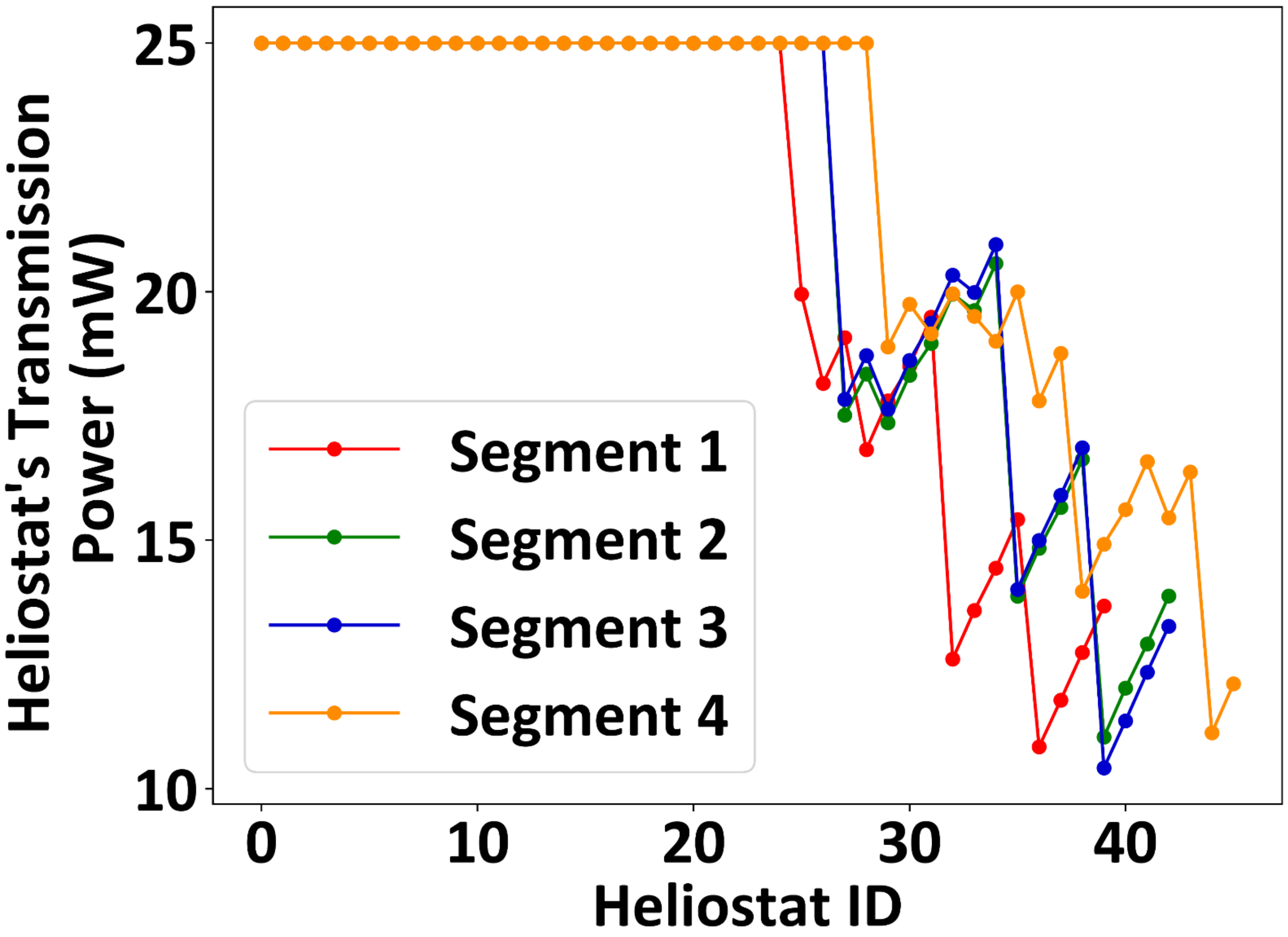

Univ of New Mexico RFP 38488-002
Simulation Results

Energy Efficiency

- The **higher the transmission power**, the **lower** is the achieved **energy efficiency**. Hence, the downward trend of transmitting power results in an upward trend for the energy efficiency.

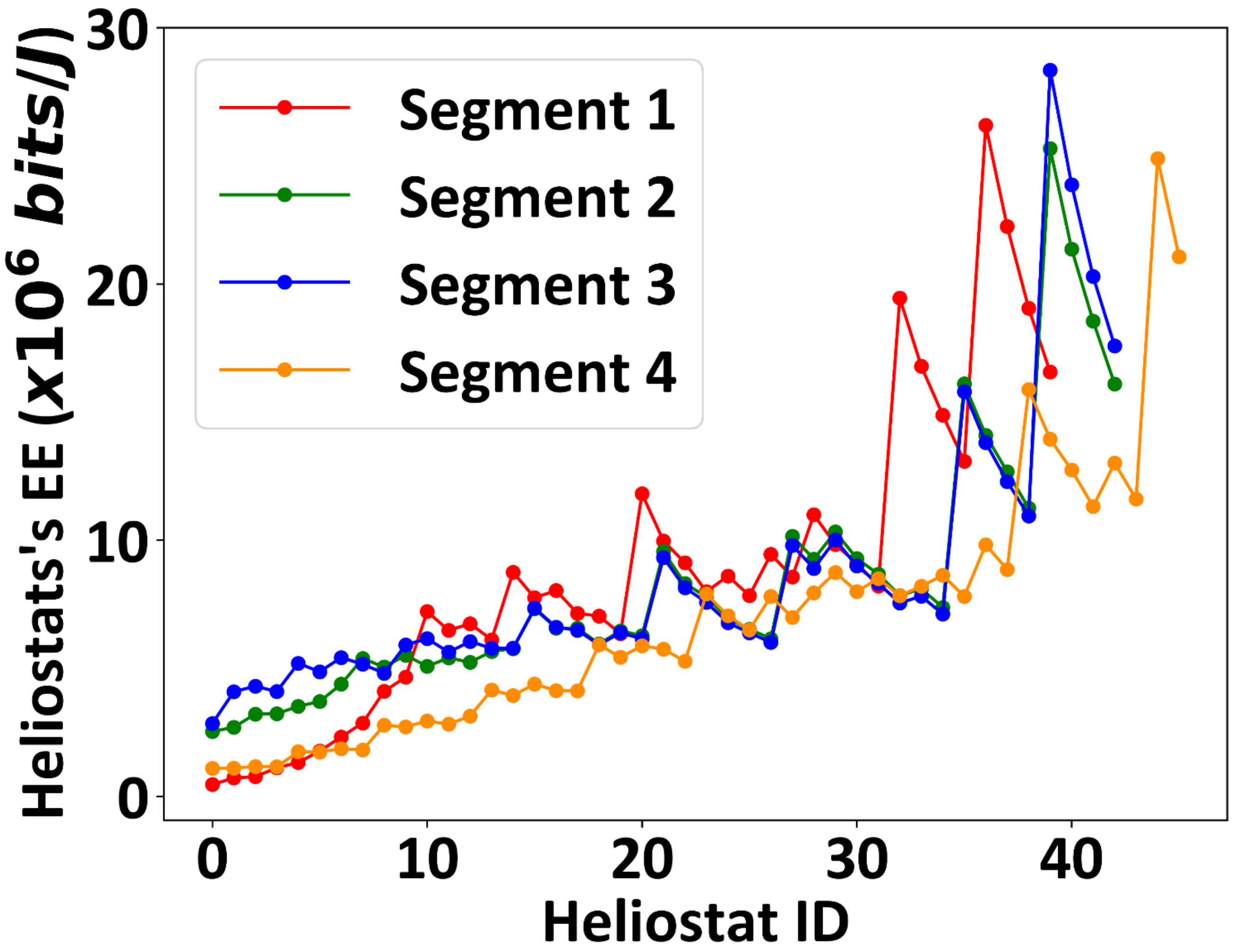

Univ of New Mexico RFP 38488-002
Current State of Research

Latency

- Any heliostat in a segment whose IAB node uses solely its backhaul for transmitting the data of its heliostats, i.e., not acting as a relaying AP, performs better in terms of latency as the entire forwarding backhaul link is dedicated to the heliostats of the specific segment.

- **Segments 1 and 2 have no backhaul links** to relay traffic coming from other segments, hence, the heliostats in those segments experience **lower latency**.

- Segments 3 and 4 both have backhaul connections, resulting in 43(heliostats)+ 2(backhaul) = 45 total connections and 46(heliostats) + 1(backhaul) = 47 total connections, respectively, resulting in a higher latency for the heliostats in segment 4.

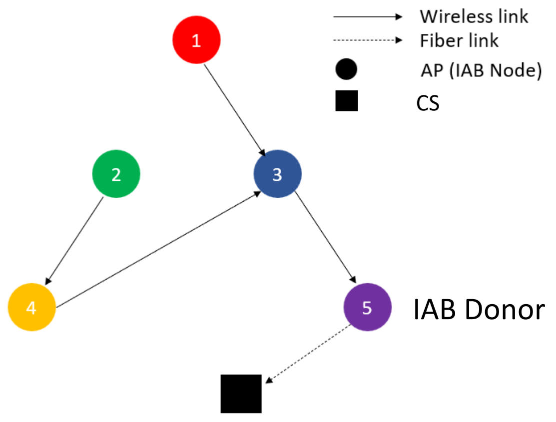

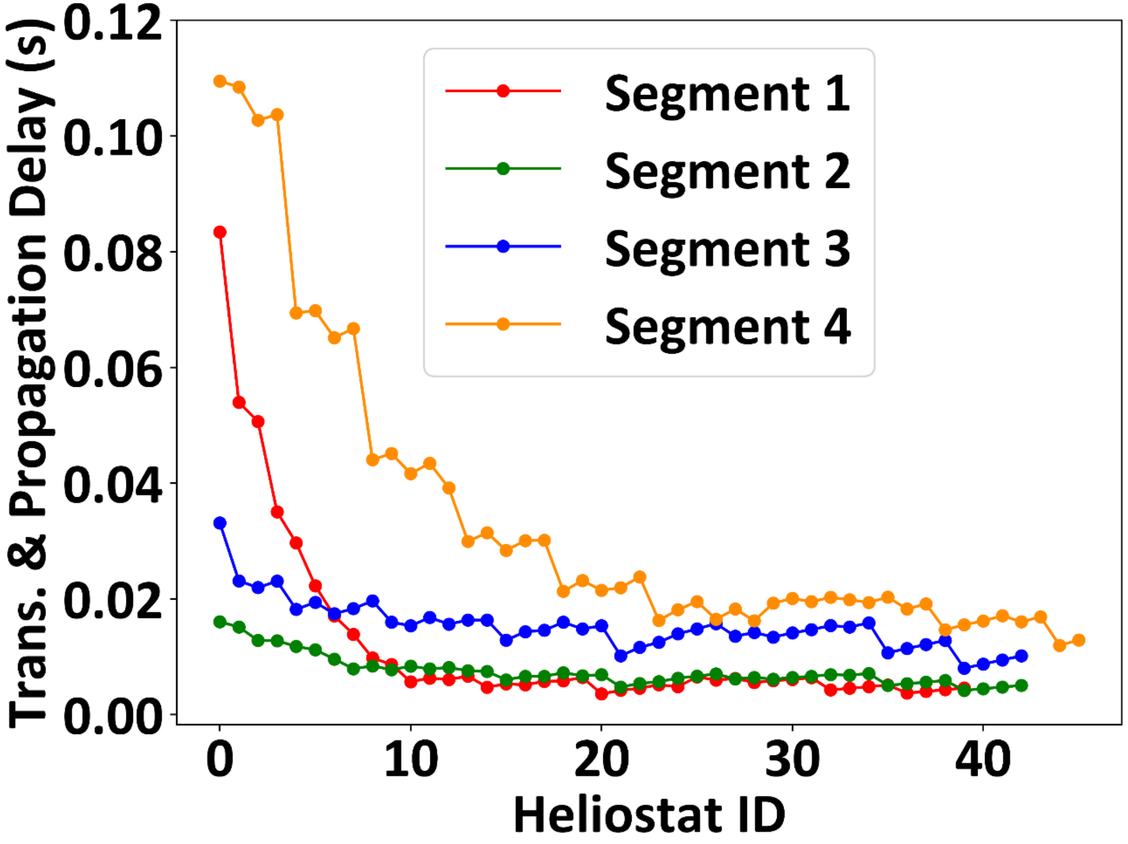

Univ of New Mexico RFP 38488-002
Simulation Results

IAB Node Transmission Power

- In order to transmit the data collected from the heliostats, all the IAB nodes are required to transmit with the maximum transmission power, i.e., 25 mW, as indicated by the hardware specs of the wireless modules (TI CC1312R or TI CC1352R).

- The optimization problem is solved with the constraint of maintaining a received power above or equal to the receiver sensitivity (critical constraint to be able to decode the received signal).

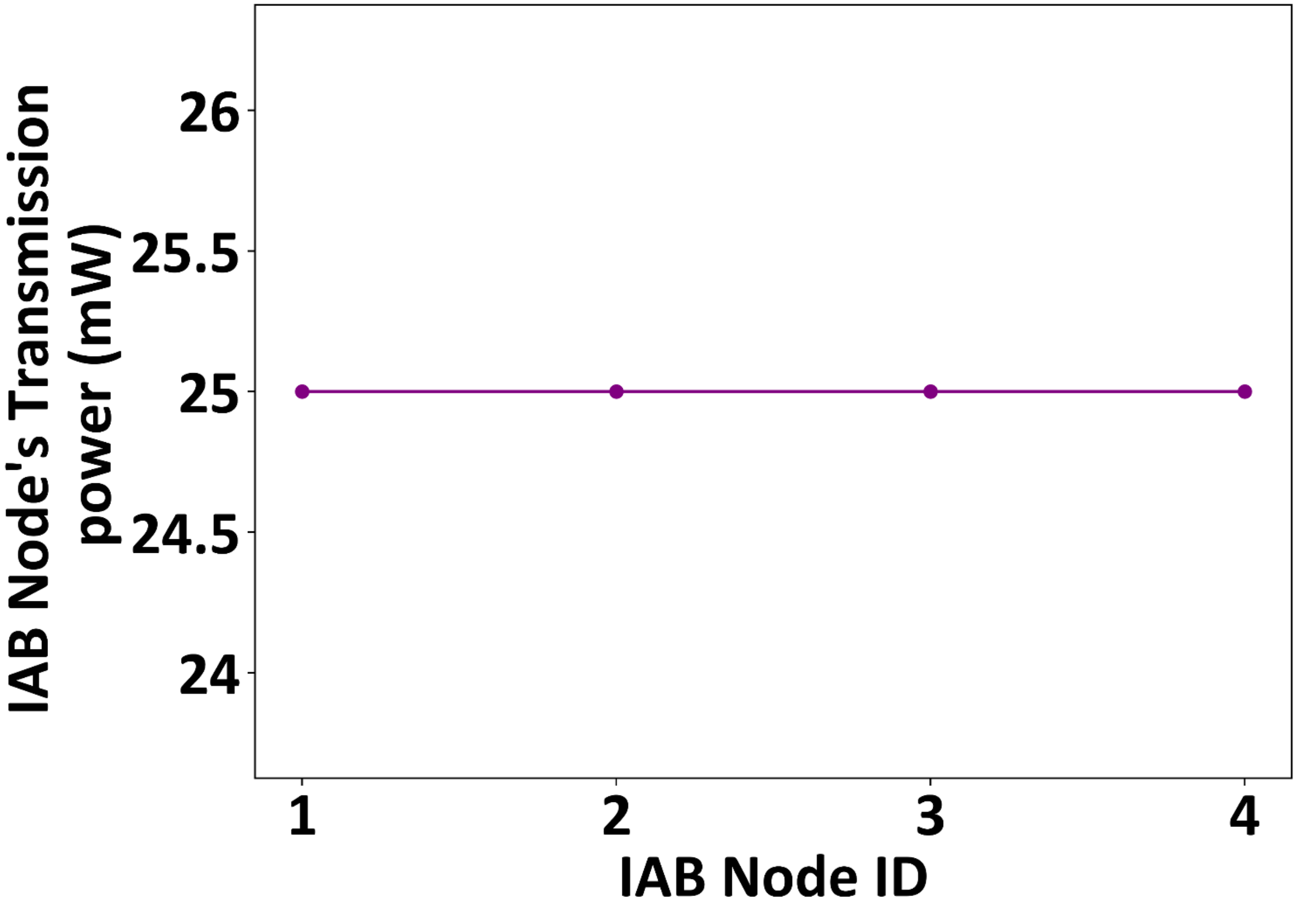

Univ of New Mexico RFP 38488-002
Simulation Results

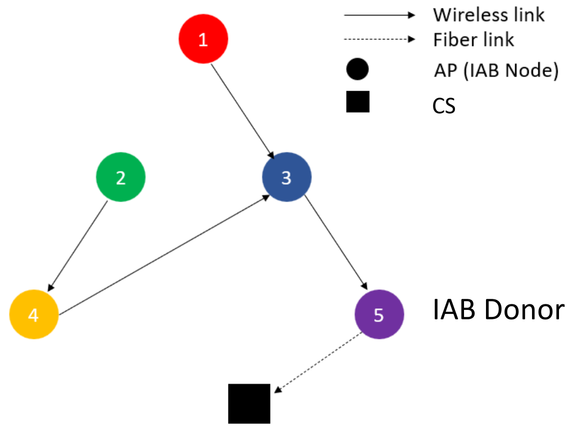

IAB Node Energy Efficiency

- **IAB nodes 1 and 2** have **higher EE** as both the APs only **serve the heliostats in the cluster and have no backhaul connections**. However, IAB Node 2 has larger number of heliostats in its access compared to IAB Node 1, hence the EE of IAB node 2 is lower than IAB node 1.

- IAB nodes 3 and 4 both have backhaul connections, resulting in 43 (heliostats) + 2 (backhaul) = 45 total connections and 46 (heliostats) + 1 (backhaul) = 47 total connections, respectively, resulting in lower EE.

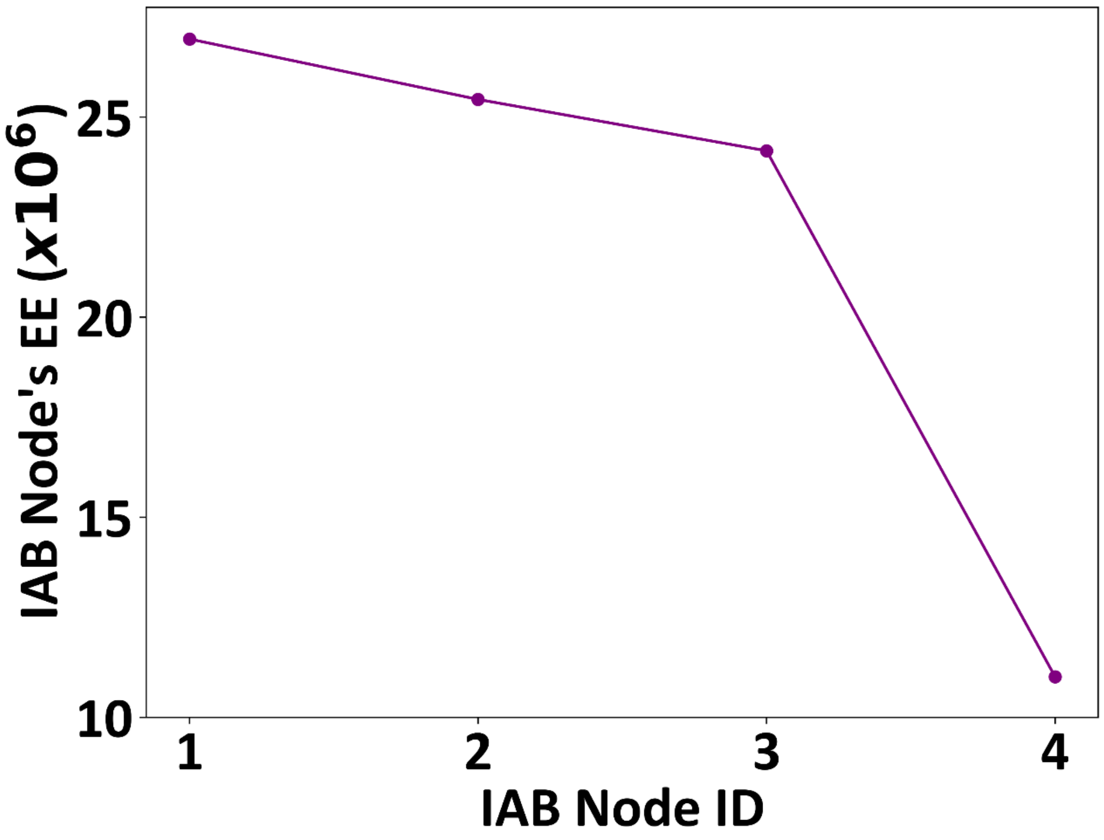

Univ of New Mexico RFP 38488-002
Simulation Results

Backhaul Rates

- The achievable data rates in the backhaul depend on the channel through which the data propagate.
- In the current topology, the **path loss in the channel between 4 and its next hop destination, i.e., 3 is the maximum, resulting in the lowest backhaul rate.**
- In the current topology, **the path loss in the channel between 1 and its next hop destination, i.e., 3 is the second maximum, resulting in the second lowest backhaul rate.**
- Given the symmetrical topology, **the path loss in the channels between 2 and its next hop destination i.e., 4 and 3 and its next hop destination i.e., 5, have almost equal path loss, resulting in the similar achieved backhaul rate.**

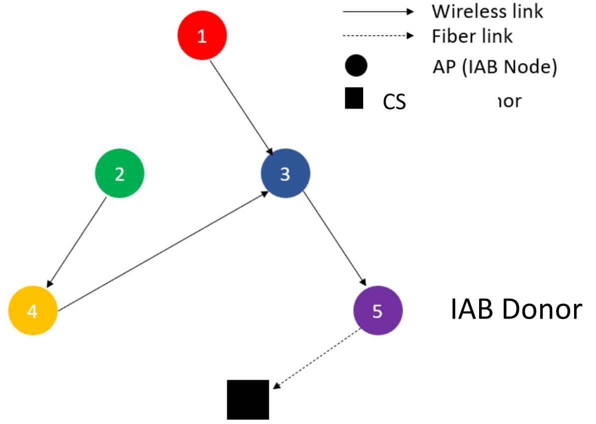

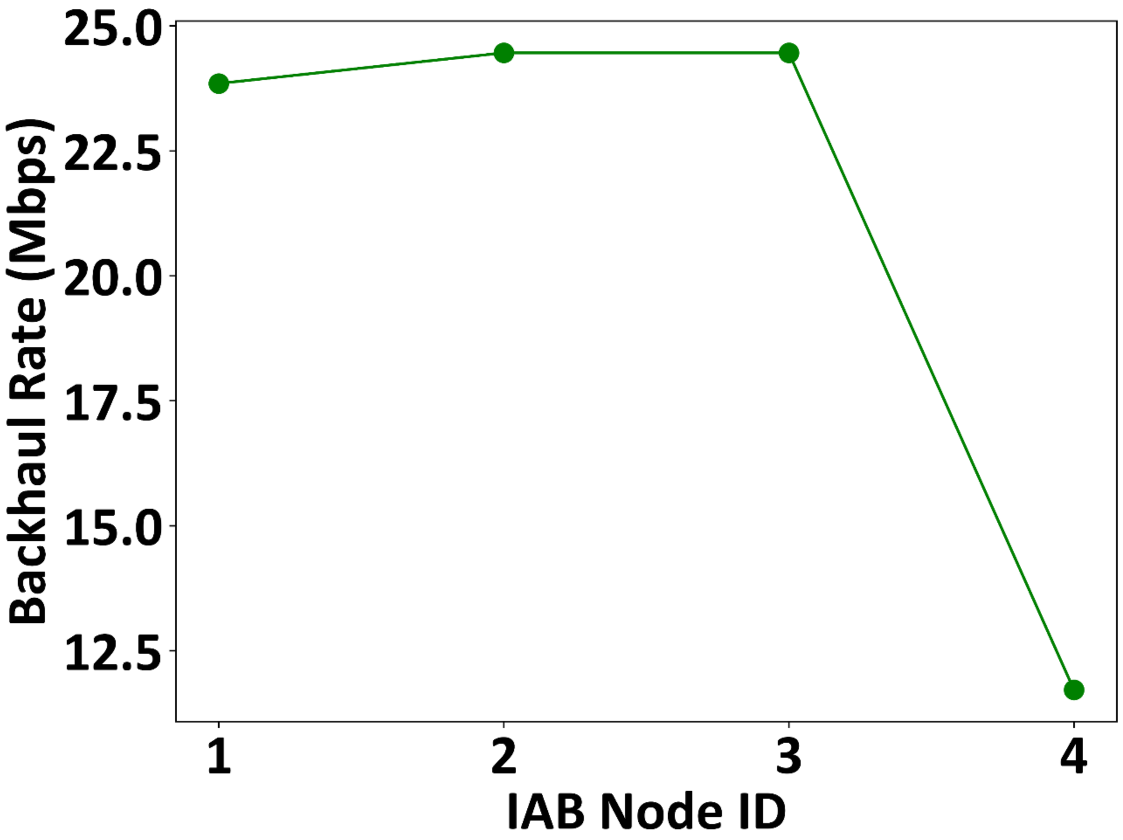

Univ of New Mexico RFP 38488-002
Emulation

OMNET++ Experiments

- Sandia's NSTTF topology is taken as the test topology to perform experiments in OMNET++ as it has a comparatively lower number of heliostats.
- A wired IAB network architecture is established initially for two major reasons.
- Wired networks can be easily and swiftly implemented in OMNET++ to analyze the communication behavior in the field.
- A wired network of the test topology can provide a basis of comparison for the emulation results obtained from the wireless implementation of the test topology.
- Testing of data transmission involves **three stages** explained as follows:
- **Uploading**: Each access heliostat uploads its data to the assigned Access Point (AP)
- **Concatenating**: Each AP processes and combines all the individual access heliostat data together
- **Forwarding**: Each AP forwards its combined data to the next AP in its route
- The uploading and concatenating stages **all occur in the same timeslot**, but they are represented as discrete events in the OMNET++ visualizations.
- The timeslot for the execution of the forwarding stage can vary from AP to AP since the APs with backhaul connections are required to wait for the backhaul APs to finish executing the forwarding of data.

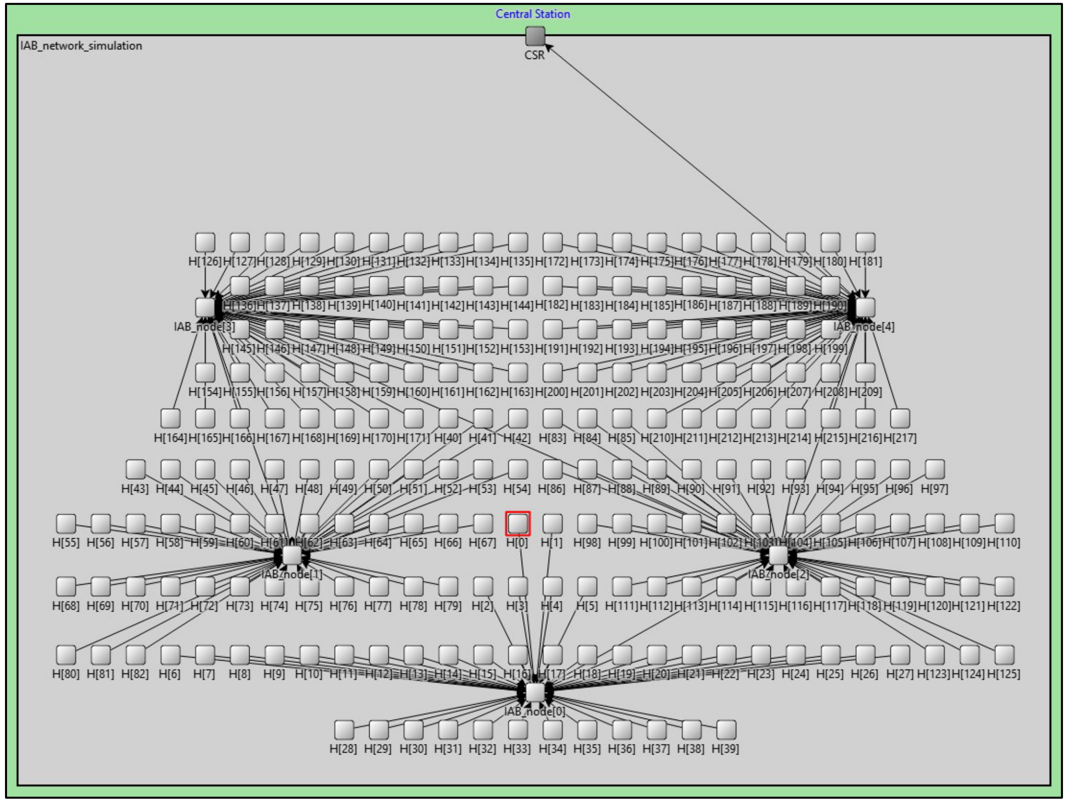

Univ of New Mexico RFP 38488-002
Emulation

Uploading stage

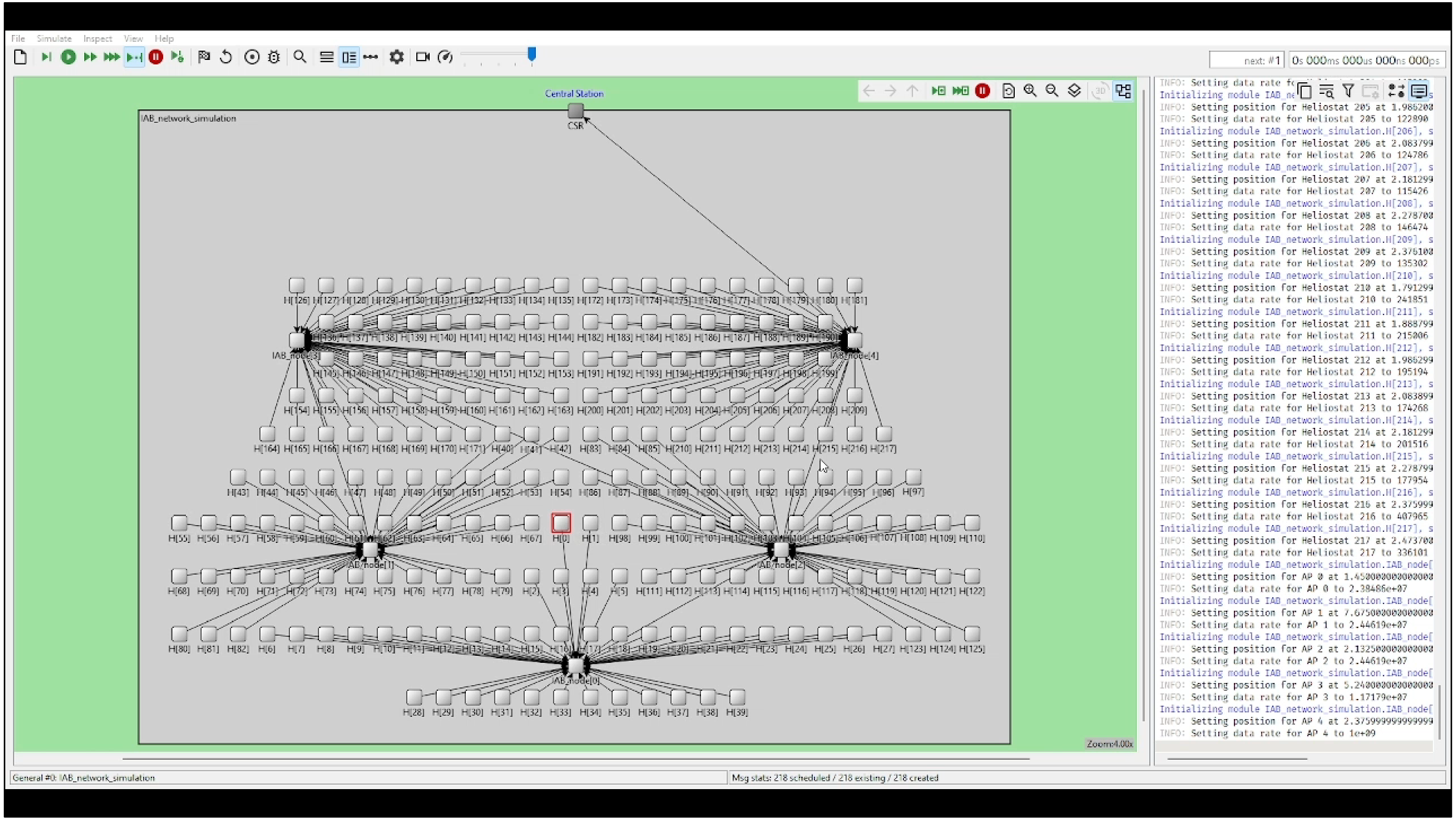

Univ of New Mexico RFP 38488-002
Emulation

Concatenating stage

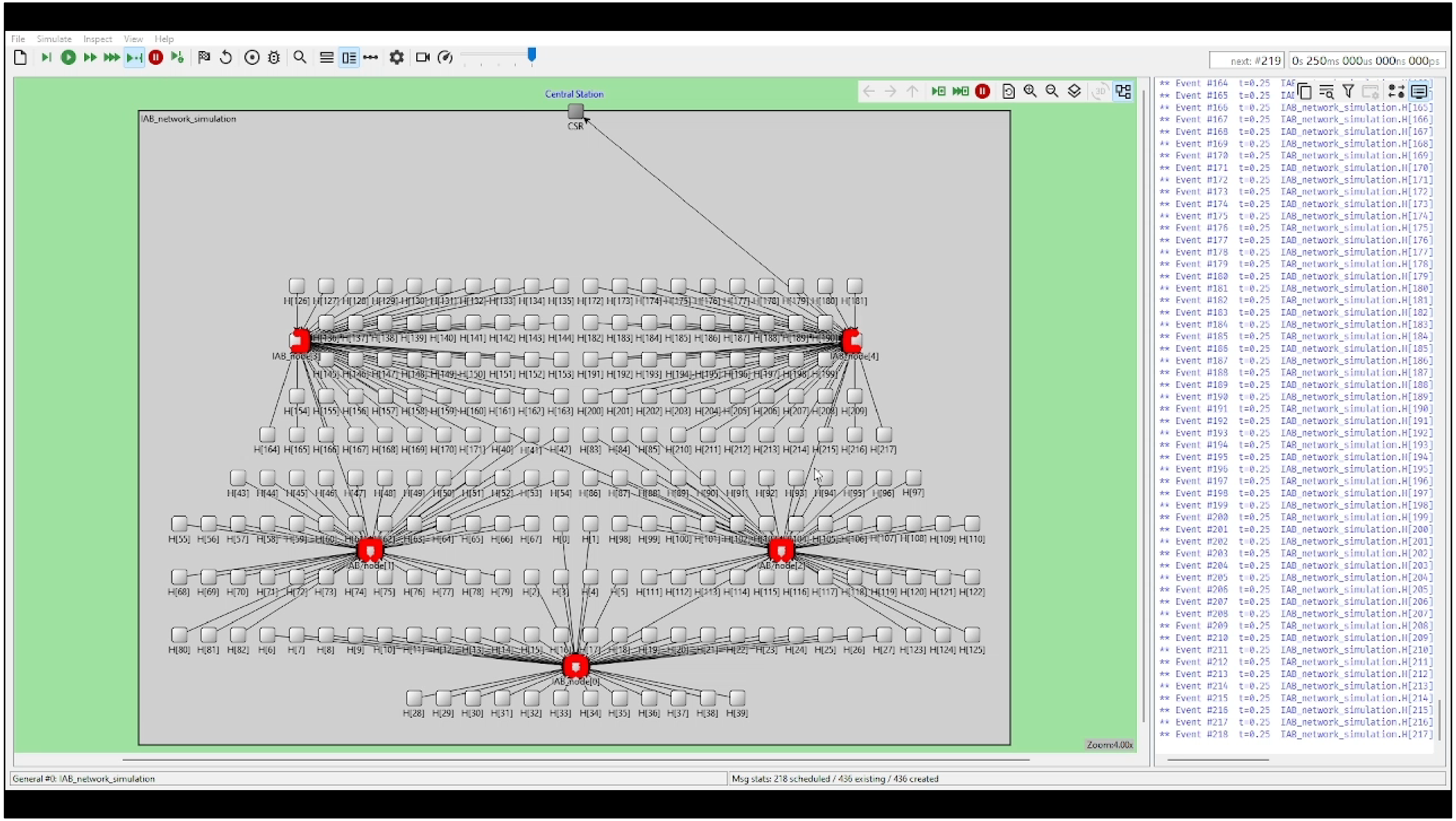

Univ of New Mexico RFP 38488-002
Emulation

Forwarding stage

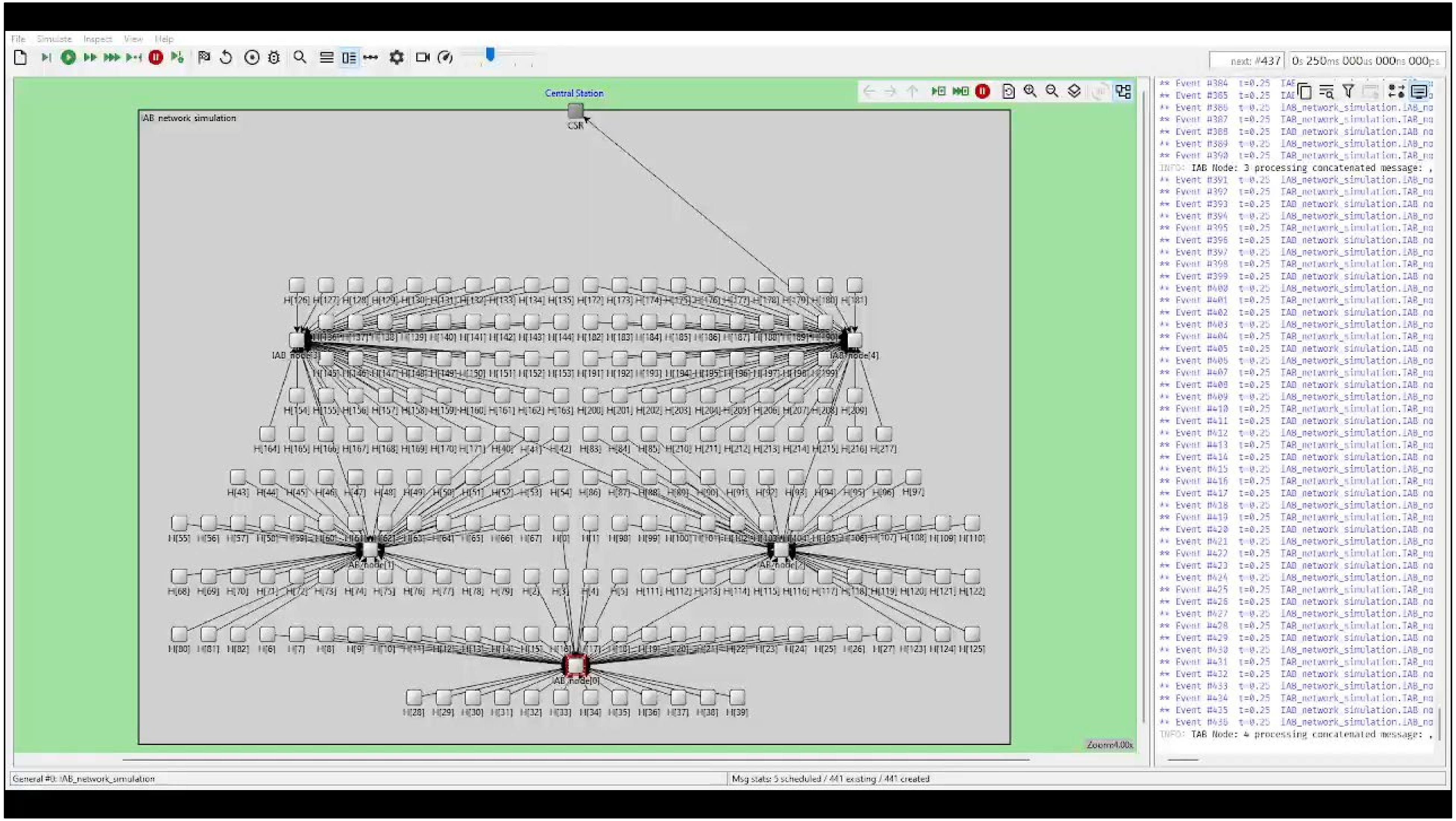

U.S. Department of Energy
HelioCon
Heliostat Consortium for
Concentrating Solar-Thermal Power

Simulation and Emulation
HELIOCON Baseline Topology @NREL

conceptional design • components • integration • mass production • heliostat field

Univ of New Mexico RFP 38488-002
Segmentation

Segmentation in NREL topology

- Heliostats are grouped into multiple segments to efficiently handle the communication among the access heliostats, IAB nodes (segment-heads) and the central station.
- Segmentation is done in two ways. Firstly, a **vertical segmentation** is done considering a fixed communication range from the central station. Then, a **horizontal segmentation** is done on top that based on the angular orientation with respect to the central station.
- Access heliostats within each segment upload their data to the associated segment-head which can forward to the next segment-head in its route or directly to the central station depending upon the routing.
- **Segment-head** is selected in a dynamic manner based on:
    - Energy availability
    - Channel gain conditions
    - Communication distance among heliostats belonging to the same segment

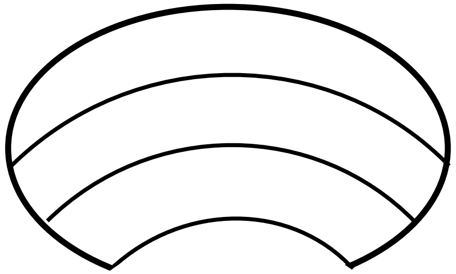

Vertical Segmentation (“arcs”)

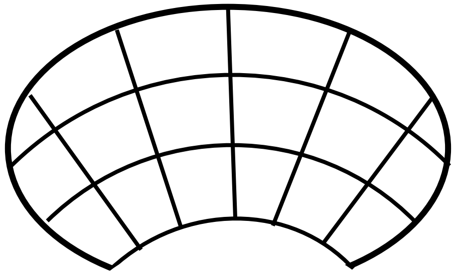

Horizontal Segmentation (“pies”)

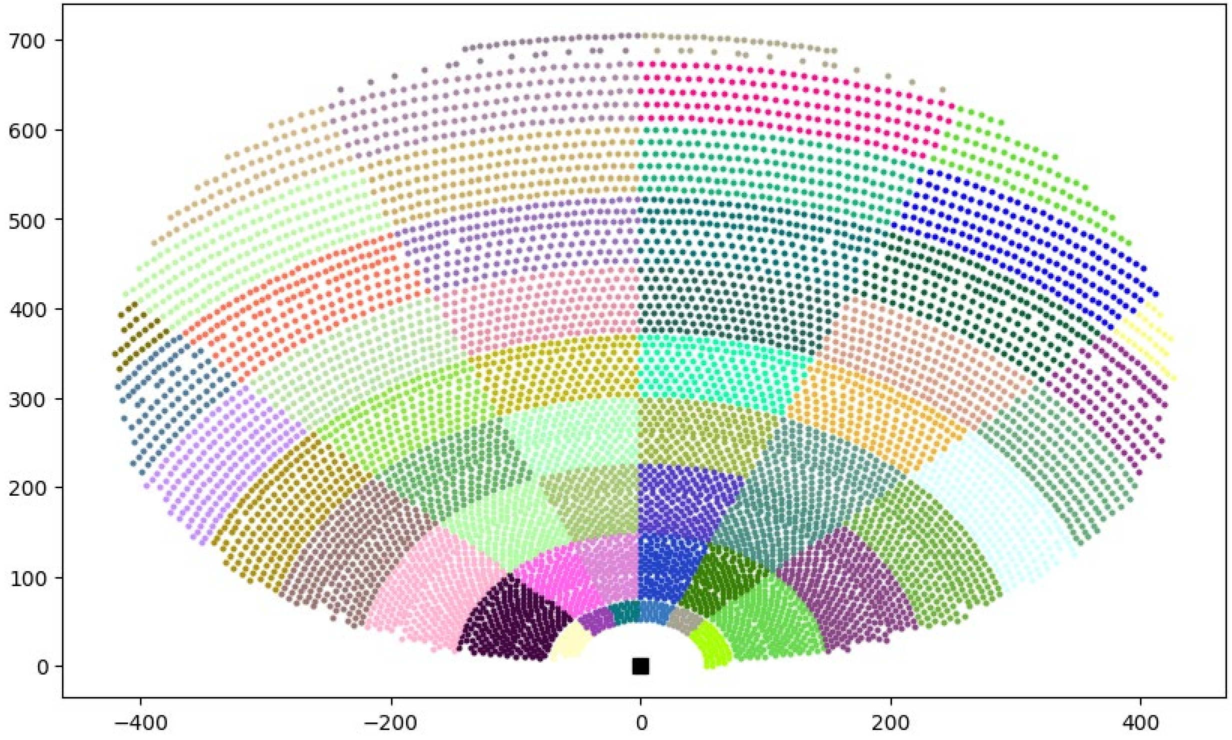

Univ of New Mexico RFP 38488-002
Segment-heads Determination

Segment-heads in NREL topology

- **Segment-heads** are determined based on the scoring criteria which is a function of the **closeness centrality and energy availability**.

- **Closeness centrality** is the average value of a combined **function of distance and channel gain**.
- Energy availability is the portion of the PV harvested energy remaining after communication operations are executed.

- Each access heliostat within a segment has a score based on the closeness centrality and energy availability and the access heliostat with the highest score is chosen to be the segment-head of the concerned segment.

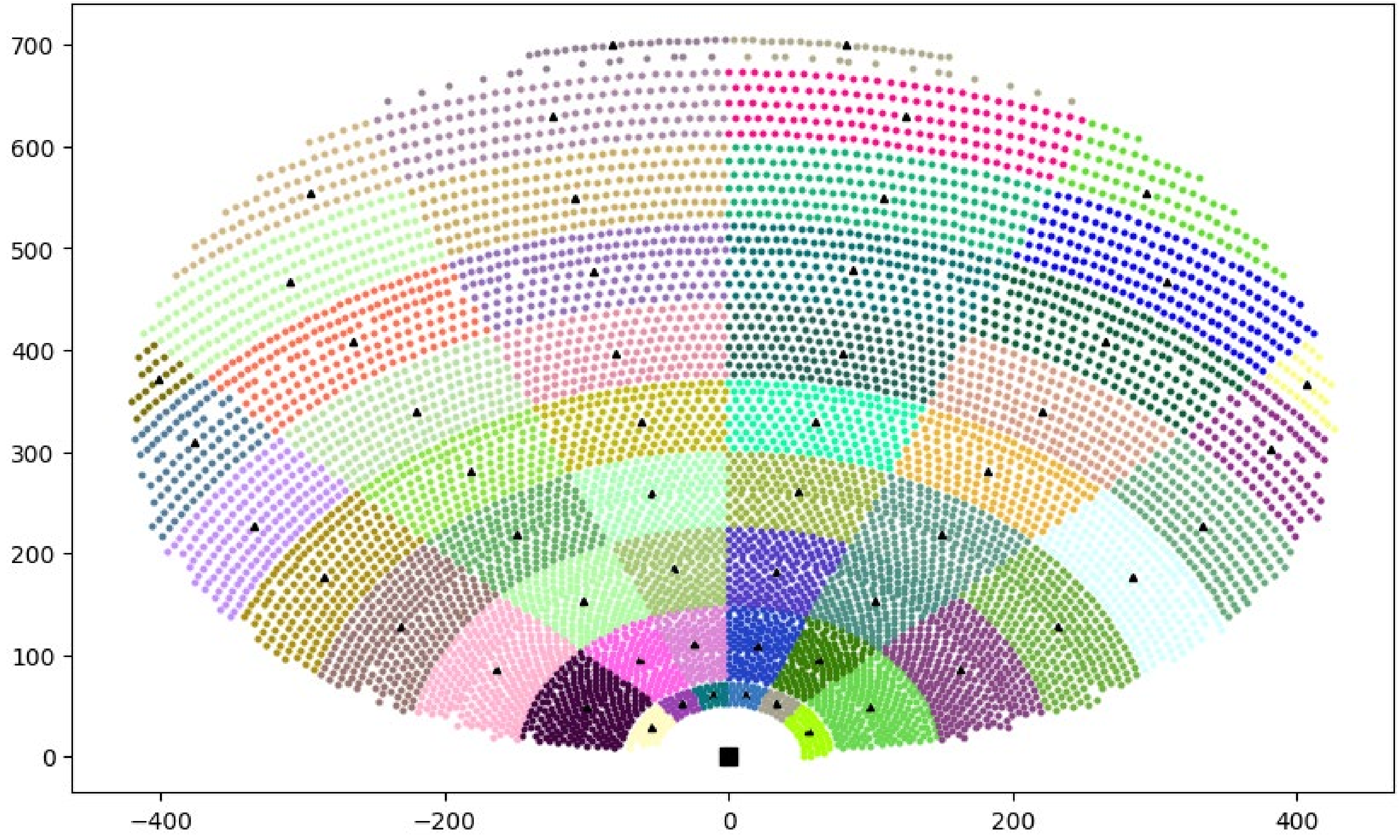

Segment-heads Determination

Segment-head Selection Process

- A segment s with heliostats denoted by $\mathcal{H}_s$ is considered.
- Segment-head selection process is initiated with the calculation of weights w_{h_s} of each heliostat h_s with other heliostats h'_s in the same segment.

$D(h_s, h'_s) = -\log_2\big(d(h_s, h'_s)\big)$, where $d(h_s, h'_s)$ is the actual **distance** between h_s and h'_s

$G(h_s, h'_s) = -\log_2(g(h_s, h'_s))$, where $g(h_s, h'_s)$ is the actual **channel gain** between h_s and h'_s

$DG(h_s, h'_s) = w_D D(h_s, h'_s) + w_G \frac{1}{G(h_s, h'_s)}$, where w_D, w_G are the weights for the distance and channel gain dependent terms respectively

$$w_{h_s}(h_s, h'_s) = DG(h_s, h'_s), \forall h'_s \in \mathcal{H}_s, h_s \neq h'_s$$

- Towards selecting the segment-head sh_s of segment s, the concept of closeness centrality CC is utilized.

$$CC(h_s) = \sum_{\substack{\forall h'_s \in \mathcal{H}_s \\ h_s \neq h'_s}} \left[\frac{w_{h_s}(h_s, h'_s)}{|\mathcal{H}_s| - 1}\right]$$

- The score of heliostat h_s as a function of closeness centrality CC and energy availability E in the segment s is defined as follows:

$score(h_s) = w_{CC} CC(h_s) + w_E \frac{E(h_s)}{E_s^{max}}$, where w_{CC}, w_E are the weights for the CC and E values respectively

- The heliostat with the highest score is the chosen segment-head: $sh_s = \underset{\forall h_s \in \mathcal{H}_s}{\operatorname{argmax}}\{score(h_s)\}$

Univ of New Mexico RFP 38488-002
Routing

Routing in NREL topology

- The **Dijkstra's algorithm** enables the determination of an **optimal route** from each segment-head to other segment-heads in its next hop, terminating at the central station.
- Dijkstra's algorithm ensures that an end-to-end path is determined from each segment-head to the central station.
- The basis for finding the optimal route in Dijkstra's algorithm is to determine the optimal route with the **minimum value of the cost function**.
- In our application of the Dijkstra's algorithm, the cost function is the **path loss** between a pair of segment-heads or between a segment-head and the central station.
- In addition, we also ensure that a segment-head has the central station as the final destination in its optimal route by ensuring that a segment-head only chooses other segment-heads in the segments which are comparatively closer to the central station.

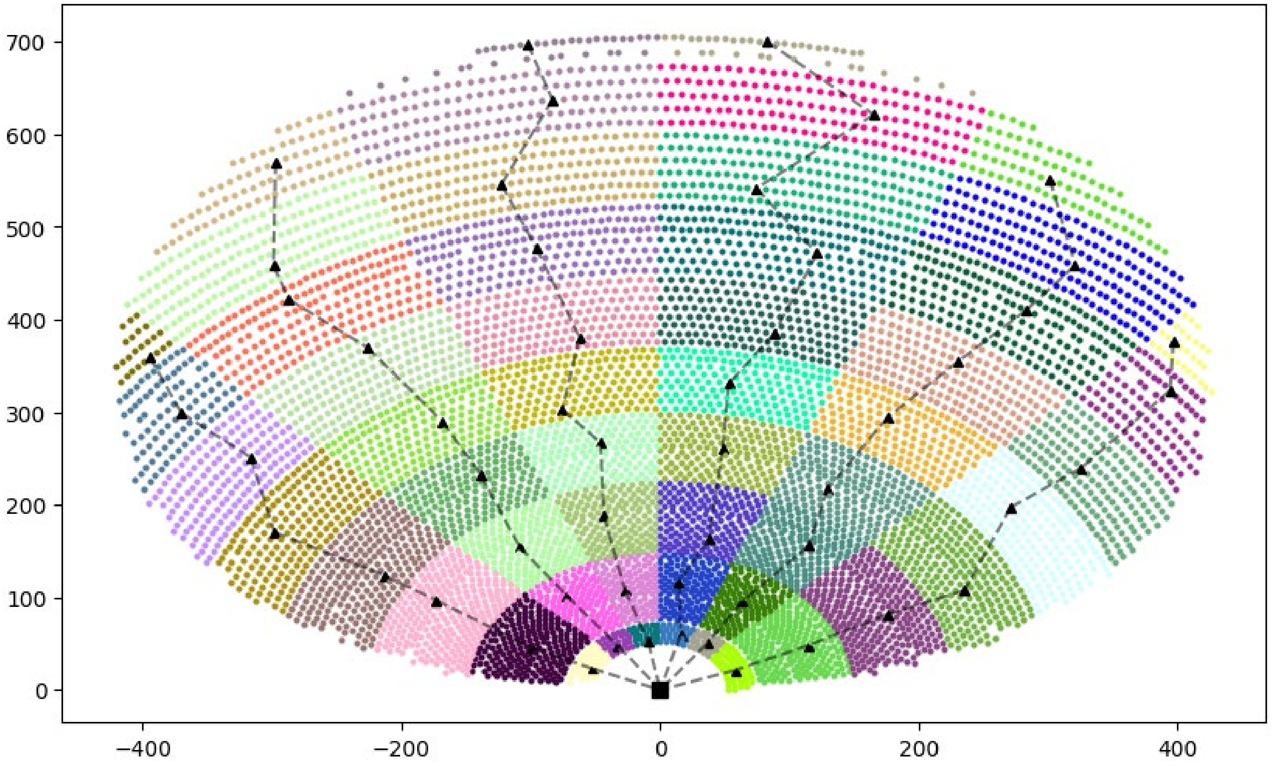

Univ of New Mexico RFP 38488-002
Energy Availability Data

- Energy availability data is analyzed to get the available energy for each day.
- For a given year, a given month and a given day, energy availability data is recorded at an interval of 5 minutes.
- For a single day, energy availability data is found only for the time the heliostats and PV panel are functional.
- The duration of PV panels being function depends on the month being considered and typically ranges from 14 hrs 15 mins (in summer) to 9 hrs 30 mins (in winter).
- The entire dataset is compiled to a file system with the following structure:

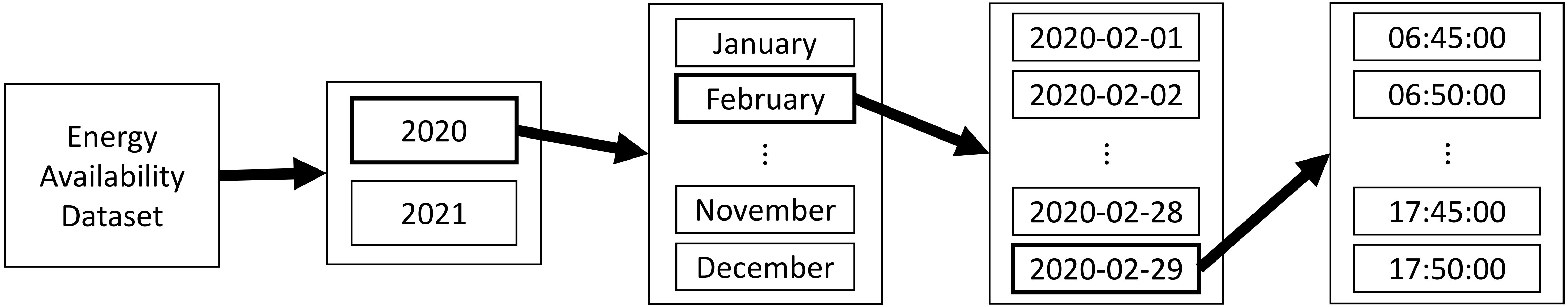

Univ of New Mexico RFP 38488-002
Energy Availability Data

- To visualize the dynamic Dijkstra routing based on the closeness centrality and energy availability, a day is chosen from the file system.
- As a representative day, 2020-07-01 is chosen as the PV panels achieve the highest duration (05:05:00 – 19:15:00) of functionality during this day.

NREL Topology
Routing Visualizations

Non-conforming heliostats

- We implemented the max EE && min latency optimization problem on the segmented Heliocon Baseline topology (7683 heliostats).
- We have considered some segments to perform closed loop autocalibration (CLA) such that the total number of heliostats performing CLA is approx. 1000, while all other remaining segments perform no closed loop autocalibration (NCLA).
- The segments performing CLA will use a different communication band from the segments performing NCLA.
- **CLA** end-to-end (E2E) latency constraint is set to **250ms**, **NCLA** E2E latency constrain set to **2s**.
- In such arrangement, we have found out a number of heliostats (approx. 1% of the total number of heliostats in the field) do not meet the latency constraints which are referred to as non-conforming heliostats.
- In attempts to solve the problem, we have further increased the segmentations (trying to imitate our future steps of clustering for Y2).
- Previously we had 54 segments, which has been increased to **108 segments** by doubling the number of "pie" divisions which is resulted in no non-conforming heliostats.

Univ of New Mexico RFP 38488-002
Simulation

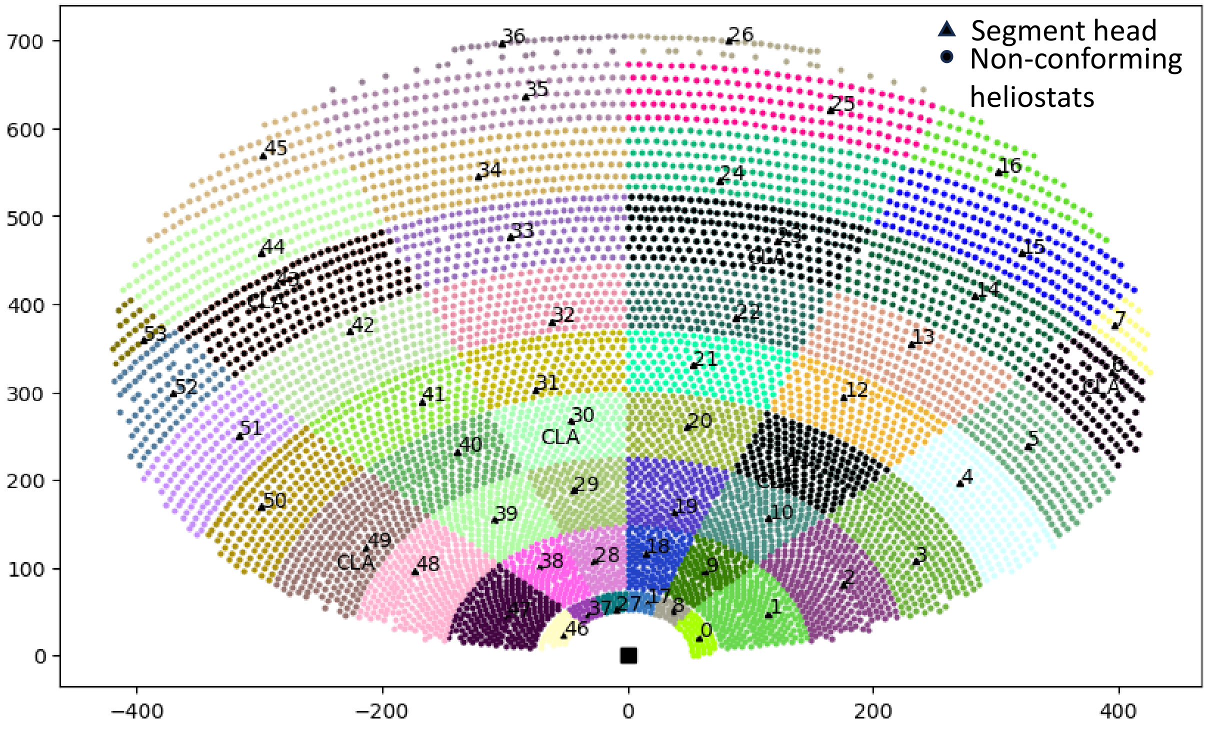

CSP field with 54 segments

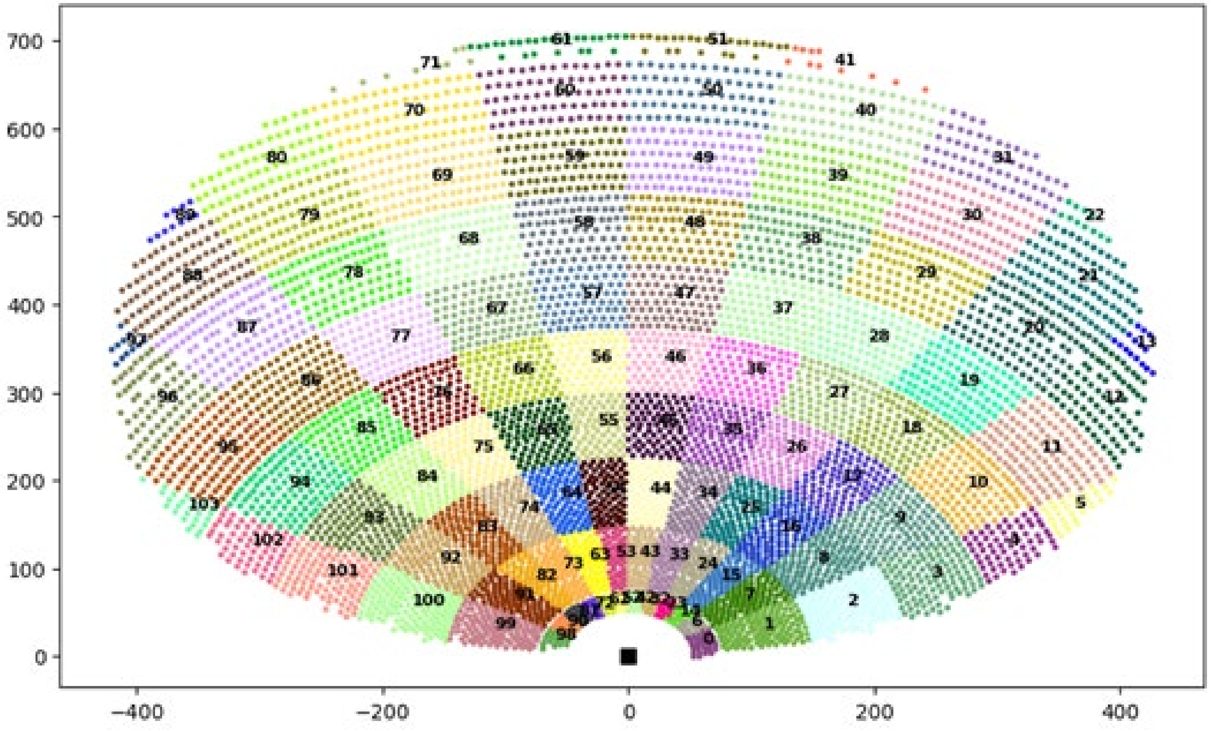

CSP field with 104 segments

Univ of New Mexico RFP 38488-002

CLA-NCLA

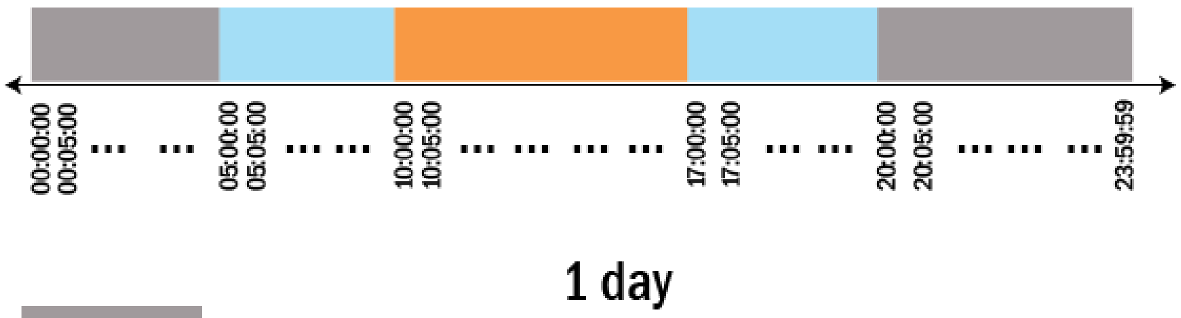

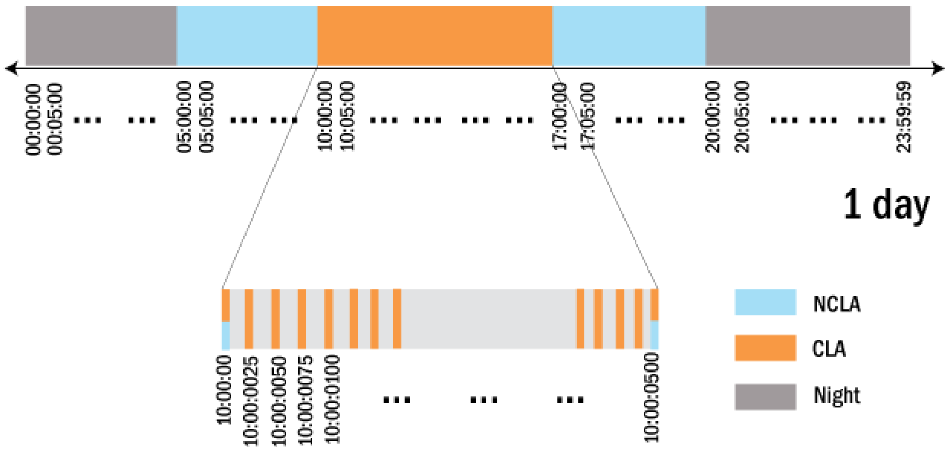

Night -- 1 signal/5 mins = 0.003 signal/sec (**sps**) with 10s *latency*. No communication, consume the very minimum of the device electronics

No closed-loop-autocalibration (N-CLA) – 1 signal/4999 msec = 0.017 **sps** with 2 sec *latency*

Closed-loop-autocalibration (CLA) – 1 signal/251 msec = 4×10^{-5} **sps** with 250 msec *latency*

- The need for CLA and NCLA transmissions at different timestamps has been identified to **prevent incidents where IAB nodes receive CLA and NCLA packets simultaneously**.
- To address this, consideration is given to adjusting the signal transmission frequencies of CLA and NCLA transmissions to **prime numbers** (**251 msec for CLA and 4999 msec for NCLA events**).
- During CLA signal transmissions, the NCLA segment heads, will function as relays, as their access networks (NCLA) will be in sleep mode during CLA transmission, and vice versa.
- To accommodate these "relay" IAB nodes, which only serve CLA segments in their backhaul connections during CLA events and vice versa during NCLA events, modifications to the maximization problem of energy efficiency and latency minimization have been concluded.

Grouping of CLA Segments

- To perform closed-loop autocalibration (CLA), we are required to group multiple segments in the heliostats field and all the heliostats within each segment of the group will perform CLA simultaneously.

- The heliostats performing the CLA will operate in a separate frequency band (TI Module page-14) compared to the heliostats not performing CLA (NCLA segments/groups).

- The **segments in a CLA group** should be chosen in such a way that they **do not interfere** with each other and so that all the heliostats can achieve the strict CLA time constraint.

- The interference region of a heliostat operating with **Zigbee** protocol is **75 m** on an average. So, the minimum distance among all the segments in a CLA group should be more than 75 m to avoid any associated interferences.

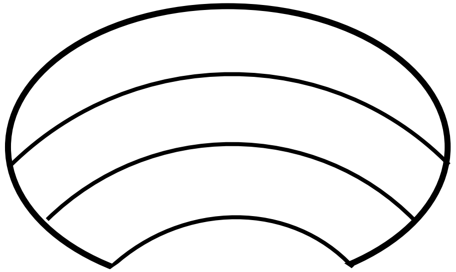

Vertical Segmentation ("arcs")

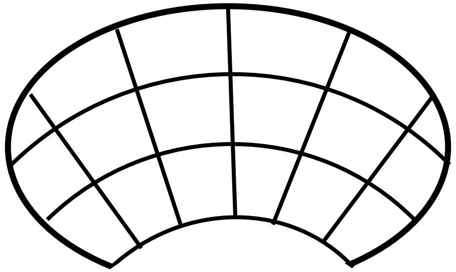

Horizontal Segmentation ("pies")

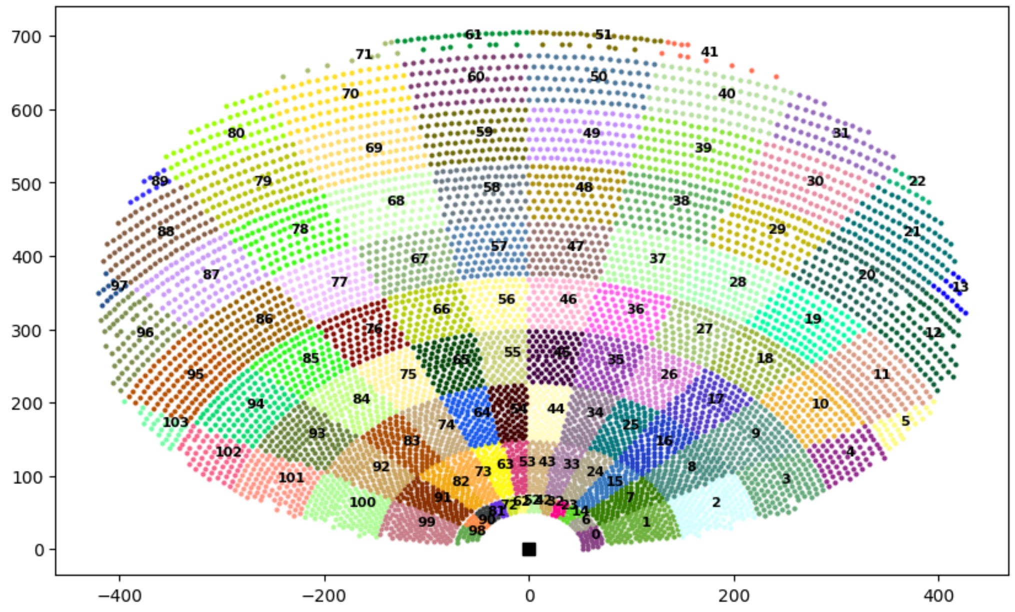

Univ of New Mexico RFP 38488-002
CLA-NCLA

Grouping of CLA Segments – Approach 1

- We start with the segments **sequentially from each arc** and each segment is allowed to choose another segment from the same arc sequentially to form a group.
- Each of the segments in the first arc form CLA groups in a sequential manner and **then we move to the** segments in the **next arc** (towards the edge of the field).
- A segment that has already been included in a CLA group is not considered when another CLA group is formed. So, the algorithm takes the lowest id non-grouped segments from arcs sequentially each time a CLA group must be formed.
- The algorithm terminates when there are no new groups that can be formed.

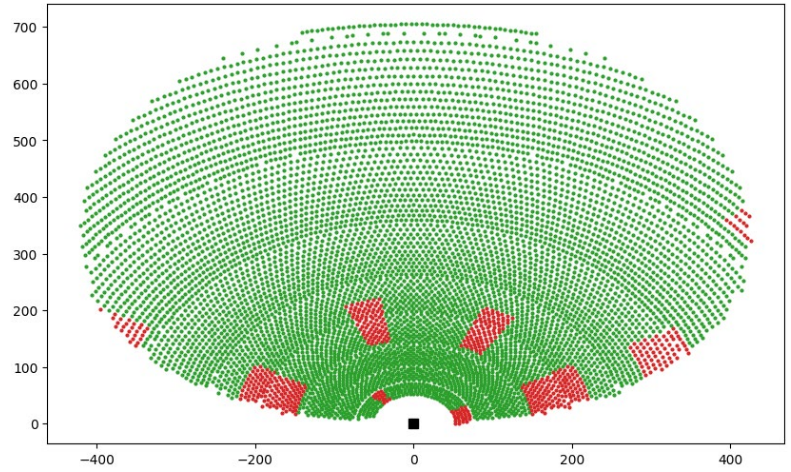

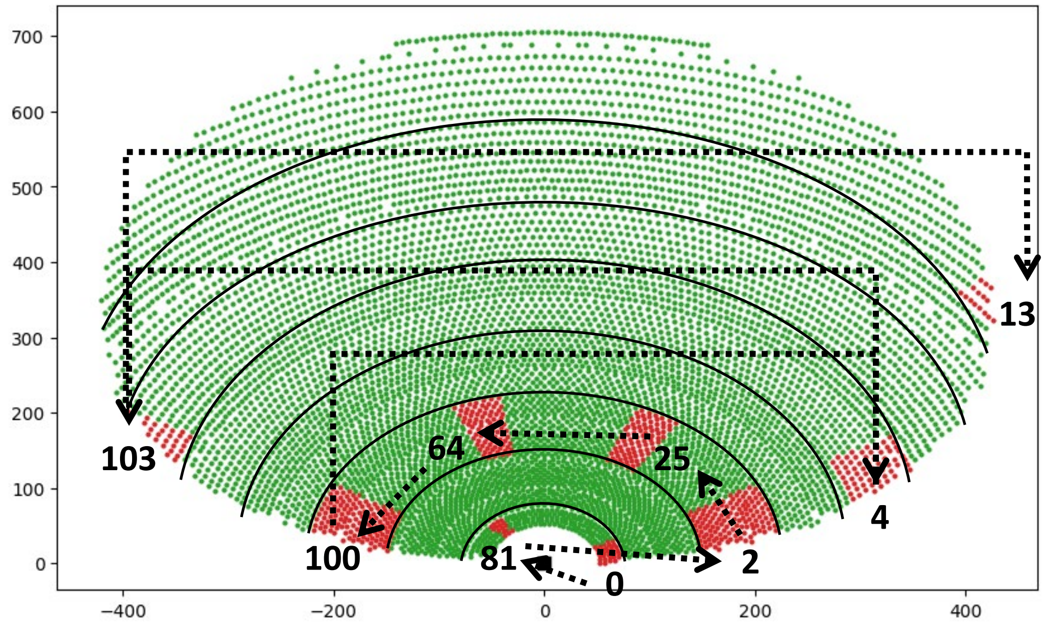

CLA Group 1: [0, 81, 2, 25, 64, 100, 4, 103, 13]

Grouping of CLA Segments – Approach 1 Outcomes

(a) Total Number of Heliostats in a CLA group: ~1000

```
CLA Group 1 Segment IDs: [0, 81, 2, 25, 64, 100, 4, 18, 46, 76, 102, 12, 97, 22, 89, 41, 71]
CLA Group 1 Heliostat Number: 991
CLA Group 2 Segment IDs: [6, 90, 8, 44, 83, 10, 36, 66, 94, 20, 38, 58]
CLA Group 2 Heliostat Number: 989
CLA Group 3 Segment IDs: [14, 98, 16, 54, 92, 27, 56, 85, 5, 103, 29, 48, 68, 87]
CLA Group 3 Heliostat Number: 990
CLA Group 4 Segment IDs: [23, 91, 34, 3, 65, 93, 11, 28, 47, 77, 96, 13]
CLA Group 4 Heliostat Number: 979
CLA Group 5 Segment IDs: [32, 99, 74, 9, 35, 101, 19, 37, 67, 86, 31]
CLA Group 5 Heliostat Number: 981
CLA Group 6 Segment IDs: [42, 17, 45, 75, 57, 95, 78, 21, 39, 59, 80, 51]
CLA Group 6 Heliostat Number: 929
CLA Group 7 Segment IDs: [52, 1, 26, 55, 84, 30, 49, 69, 88, 61]
CLA Group 7 Heliostat Number: 787
CLA Group 8 Segment IDs: [62, 79, 40, 60]
CLA Group 8 Heliostat Number: 260
CLA Group 9 Segment IDs: [72, 7, 50, 70]
CLA Group 9 Heliostat Number: 256
CLA Group 10 Segment IDs: [15, 73]
CLA Group 10 Heliostat Number: 136
CLA Group 11 Segment IDs: [24, 82]
CLA Group 11 Heliostat Number: 136
CLA Group 12 Segment IDs: [33]
CLA Group 12 Heliostat Number: 68
CLA Group 13 Segment IDs: [43]
CLA Group 13 Heliostat Number: 62
CLA Group 14 Segment IDs: [53]
CLA Group 14 Heliostat Number: 51
CLA Group 15 Segment IDs: [63]
CLA Group 15 Heliostat Number: 68
-------------------------------------------------------------
Total Number of Heliostats performing CLA: 7683
```

(a)
Groups: 15 →
150 min CLA
Standalones: 4
Less Balanced

(b) Total Number of Heliostats in a CLA group: ~600

```
CLA Group 1 Segment IDs: [0, 81, 2, 25, 64, 100, 4, 103, 13]
CLA Group 1 Heliostat Number: 596
CLA Group 2 Segment IDs: [6, 90, 8, 44, 83, 10, 36, 102, 97]
CLA Group 2 Heliostat Number: 597
CLA Group 3 Segment IDs: [14, 98, 16, 54, 92, 18, 46, 76, 5]
CLA Group 3 Heliostat Number: 599
CLA Group 4 Segment IDs: [23, 91, 34, 3, 65, 93, 27, 71]
CLA Group 4 Heliostat Number: 600
CLA Group 5 Segment IDs: [32, 99, 74, 9, 35, 101, 96]
CLA Group 5 Heliostat Number: 599
CLA Group 6 Segment IDs: [42, 17, 45, 75, 11, 28, 47, 22, 89]
CLA Group 6 Heliostat Number: 591
CLA Group 7 Segment IDs: [52, 1, 26, 55, 84, 19, 37, 41]
CLA Group 7 Heliostat Number: 594
CLA Group 8 Segment IDs: [62, 56, 85, 12, 29, 48, 68, 31]
CLA Group 8 Heliostat Number: 580
CLA Group 9 Segment IDs: [72, 7, 66, 94, 20, 38, 58, 51]
CLA Group 9 Heliostat Number: 595
CLA Group 10 Segment IDs: [15, 73, 57, 77, 95, 21, 40]
CLA Group 10 Heliostat Number: 598
CLA Group 11 Segment IDs: [24, 82, 67, 86, 30, 49, 70]
CLA Group 11 Heliostat Number: 595
CLA Group 12 Segment IDs: [33, 78, 39, 59, 80, 61]
CLA Group 12 Heliostat Number: 430
CLA Group 13 Segment IDs: [43, 87, 69, 50]
CLA Group 13 Heliostat Number: 330
CLA Group 14 Segment IDs: [53, 79, 60]
CLA Group 14 Heliostat Number: 217
CLA Group 15 Segment IDs: [63, 88]
CLA Group 15 Heliostat Number: 162
-------------------------------------------------------------
Total Number of Heliostats performing CLA: 7683
```

(b)
Groups: 15 →
150 min CLA
Standalones: 0
More Balanced

CLA Segments with Approach 1 (Total Number of Heliostats in a CLA group: ~ 600)

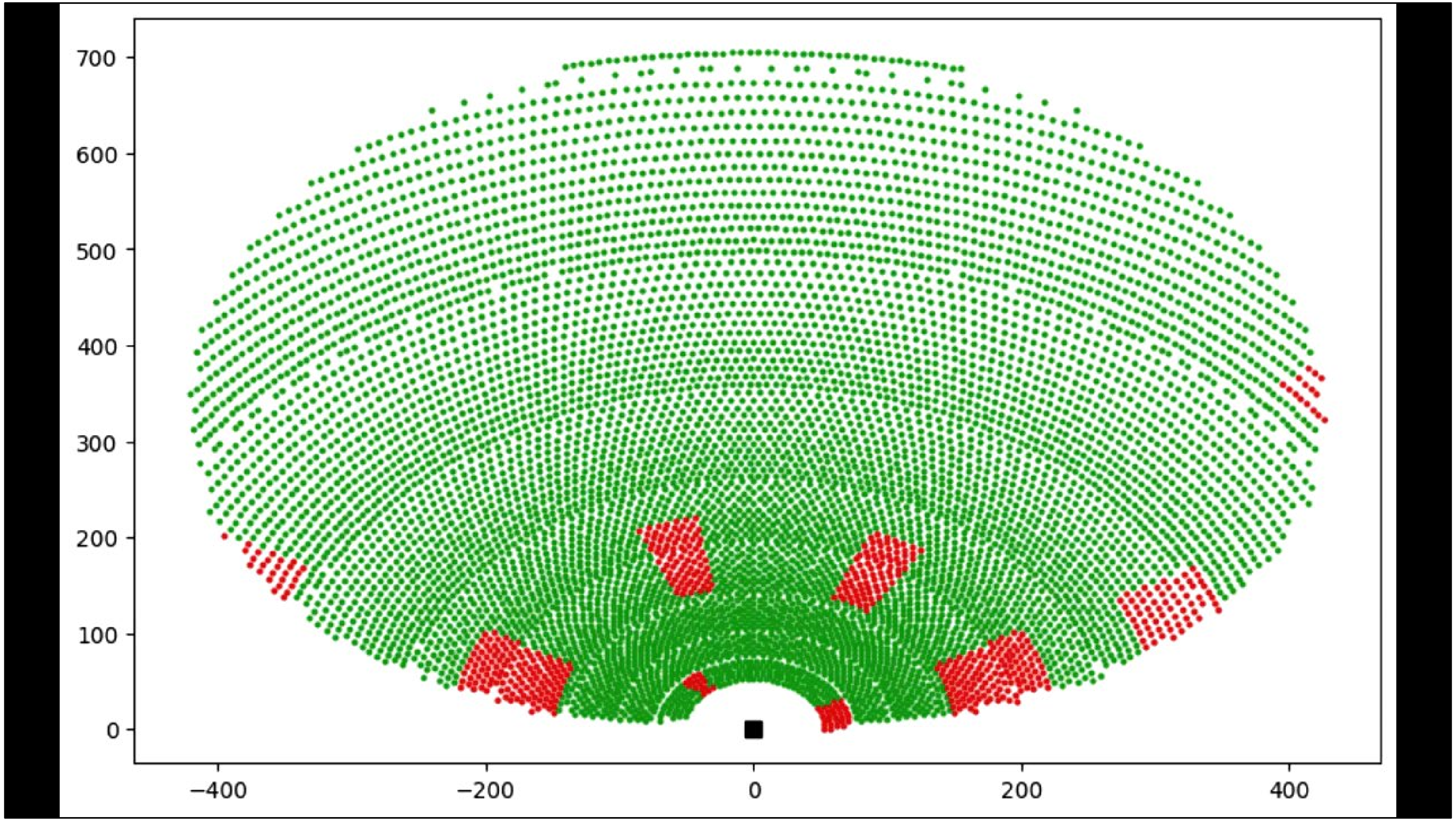

Univ of New Mexico RFP 38488-002
CLA-NCLA

Grouping of CLA Segments – Approach 2

- We start with the segments **sequentially from the first arc** and each segment is allowed to **choose another lowest id non-grouped segment from the pies**.
- Each of the segments in the arcs form CLA groups in a sequential manner and then we move to the segments in the next arc.
- A segment that has been included in a CLA group is not considered when another CLA group is formed. So, the algorithm takes the lowest id non-grouped segments from the pies sequentially each time a CLA group must be formed.
- The algorithm terminates when there are no new groups that can be formed.

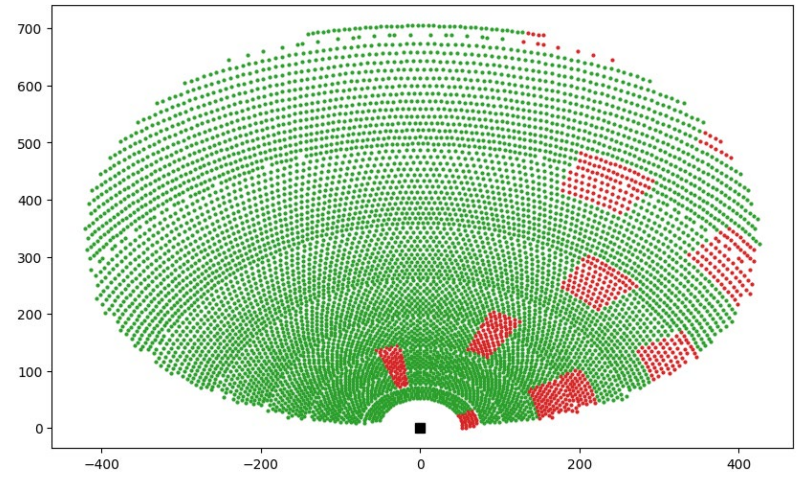

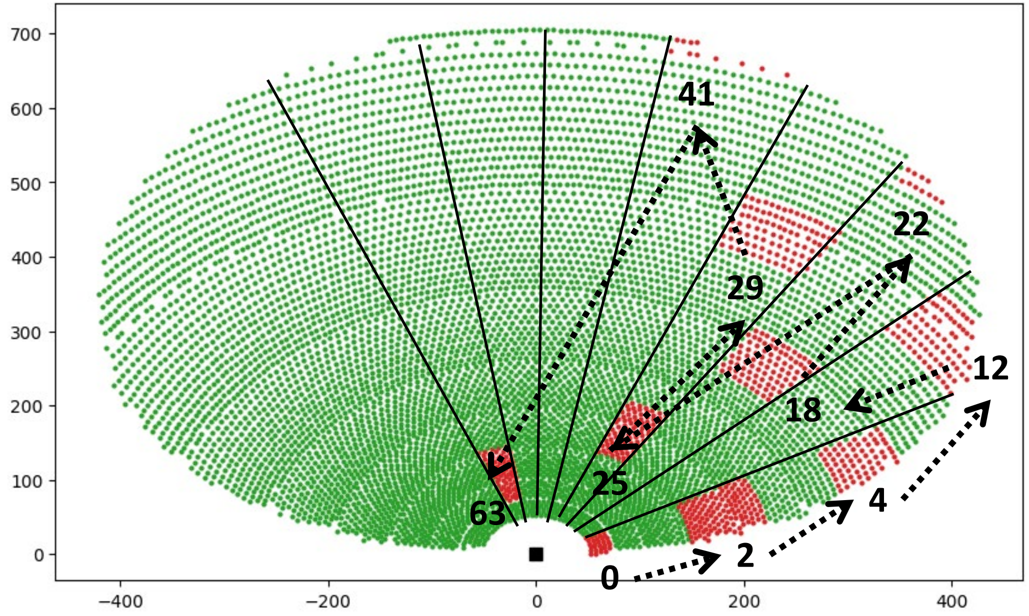

CLA Group 1: [0, 2, 4, 12, 18, 22, 25, 29, 41, 63]

Grouping of CLA Segments – Approach 2 Outcomes

(a) Total Number of Heliostats in a CLA group: ~1000

```
CLA Group 1 Segment IDs: [0, 2, 4, 12, 18, 22, 25, 29, 40, 46, 48, 60, 63, 89, 97]
CLA Group 1 Heliostat Number: 983
CLA Group 2 Segment IDs: [6, 3, 5, 13, 19, 26, 30, 37, 41, 49, 54, 61, 66, 68, 80]
CLA Group 2 Heliostat Number: 996
CLA Group 3 Segment IDs: [14, 8, 10, 20, 31, 35, 38, 50, 57, 64, 69, 71, 96]
CLA Group 3 Heliostat Number: 1000
CLA Group 4 Segment IDs: [23, 9, 11, 21, 28, 34, 39, 47, 51, 59, 65, 77, 91]
CLA Group 4 Heliostat Number: 1083
CLA Group 5 Segment IDs: [32, 16, 27, 55, 58, 70, 78, 83, 85, 102]
CLA Group 5 Heliostat Number: 771
CLA Group 6 Segment IDs: [42, 17, 44, 56, 79, 84, 86, 103]
CLA Group 6 Heliostat Number: 586
CLA Group 7 Segment IDs: [52, 1, 36, 67, 74, 87, 94, 100]
CLA Group 7 Heliostat Number: 731
CLA Group 8 Segment IDs: [62, 45, 75, 88, 95, 101]
CLA Group 8 Heliostat Number: 496
CLA Group 9 Segment IDs: [72, 7, 76, 92]
CLA Group 9 Heliostat Number: 300
CLA Group 10 Segment IDs: [81, 15, 93]
CLA Group 10 Heliostat Number: 199
CLA Group 11 Segment IDs: [90, 24]
CLA Group 11 Heliostat Number: 85
CLA Group 12 Segment IDs: [98, 33]
CLA Group 12 Heliostat Number: 88
CLA Group 13 Segment IDs: [43, 99]
CLA Group 13 Heliostat Number: 178
CLA Group 14 Segment IDs: [53]
CLA Group 14 Heliostat Number: 51
CLA Group 15 Segment IDs: [73]
CLA Group 15 Heliostat Number: 67
CLA Group 16 Segment IDs: [82]
CLA Group 16 Heliostat Number: 69
------------------------------------------------------------------------
Total Number of Heliostats performing CLA: 7683
```

(a)
Groups: 16 →
160 min CLA
Standalones: 3
Less Balanced

(b) Total Number of Heliostats in a CLA group: ~600

```
CLA Group 1 Segment IDs: [0, 2, 4, 12, 18, 22, 25, 29, 41, 63]
CLA Group 1 Heliostat Number: 664
CLA Group 2 Segment IDs: [6, 3, 5, 13, 19, 26, 30, 37, 51, 71, 89, 73]
CLA Group 2 Heliostat Number: 666
CLA Group 3 Segment IDs: [14, 8, 10, 20, 31, 35, 38, 97, 82]
CLA Group 3 Heliostat Number: 662
CLA Group 4 Segment IDs: [23, 9, 11, 21, 28, 34, 40, 91]
CLA Group 4 Heliostat Number: 687
CLA Group 5 Segment IDs: [32, 16, 27, 39, 47, 54, 59, 61, 103]
CLA Group 5 Heliostat Number: 588
CLA Group 6 Segment IDs: [42, 17, 44, 46, 48, 50, 68, 70]
CLA Group 6 Heliostat Number: 599
CLA Group 7 Segment IDs: [52, 1, 36, 49, 64, 66, 69]
CLA Group 7 Heliostat Number: 572
CLA Group 8 Segment IDs: [62, 45, 57, 60, 74, 76, 78, 80]
CLA Group 8 Heliostat Number: 569
CLA Group 9 Segment IDs: [72, 7, 55, 58, 77, 79, 83]
CLA Group 9 Heliostat Number: 545
CLA Group 10 Segment IDs: [81, 15, 56, 84, 86, 88, 102]
CLA Group 10 Heliostat Number: 510
CLA Group 11 Segment IDs: [90, 24, 65, 67, 87, 92, 94]
CLA Group 11 Heliostat Number: 588
CLA Group 12 Segment IDs: [98, 33, 75, 95, 100]
CLA Group 12 Heliostat Number: 425
CLA Group 13 Segment IDs: [43, 85, 96, 99, 101]
CLA Group 13 Heliostat Number: 443
CLA Group 14 Segment IDs: [53, 93]
CLA Group 14 Heliostat Number: 165
------------------------------------------------------------------------
Total Number of Heliostats performing CLA: 7683
```

(b)
Groups: 14 →
140 min CLA
Standalones: 0
More Balanced

CLA Segments with Approach 2 (Total Number of Heliostats in a CLA group: ~ 600)

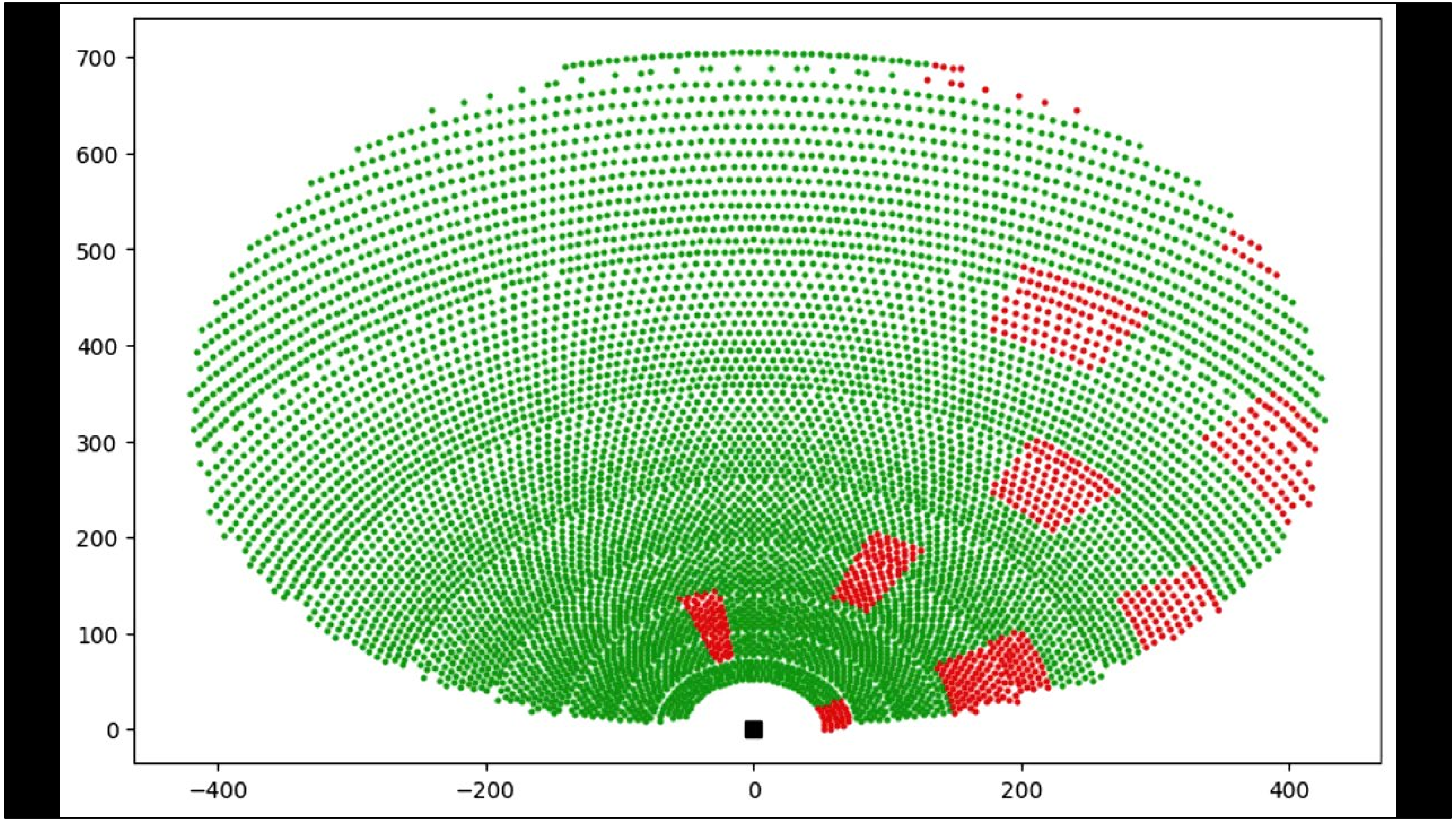

Energy Efficiency Optimization

- The heliostat field is divided into **segments** (Y2: development of clusters within segments).
- The **access heliostats** in a segment **transmit data to the segment-head**. The segment-head is responsible for forwarding the data collected from the access heliostats to the central station (CS) by following the multi-hop route identified by the **Dijkstra's algorithm** (Y2: Entropy-based routing to be developed and implemented) .
- **Segment-head** is **selected based on** an **AI-based approach** accounting for the heliostats energy availability, channel gain conditions and communication distance among each other.
- We consider a set of segments $\mathcal{C} = \{1, \ldots, c, \ldots, |\mathcal{C}|\}$, each segment having a corresponding IAB node (i.e., segment-head) N_c.
- If a segment c performs CLA with end-to-end latency constraint of 250msec, and within its route a subsequent segment c' performs NCLA with end-to-end latency constraint of 2sec, then the problem of **heterogeneous latency constraints** will arise.
- Solving an optimization problem with two different latency constraints can be computationally expensive, primarily due to the complexity of the problem, the scale of the wireless network topology, and challenges related to signal transmission synchronization.

Energy efficiency optimization for IAB nodes

- The optimization problem of the IAB nodes is formulated as follows.

$$\max_{\omega_c, P_{N_c}} EE_{N_c}(\omega_c, P_{N_c}) = \frac{R_{N_c}^{BH}}{\sum_{\forall h_c \in \mathcal{H}_c} P_{h_c} + \sum_{\forall c' \in \mathcal{N}_{N_c}^{\mathcal{BH}}} P_{N_{c'}} + P_{N_c}}$$

$$\begin{aligned} s.t.\ \boldsymbol{c1}&: 0 \leq \omega_c \leq 1 \\ \boldsymbol{c2}&: P_{N_c} \leq P^{max} \\ \boldsymbol{c3}&: P_{N_{c+1}}^{S} \geq P^{s} \\ \boldsymbol{c4}&: t_k^{E2E} \leq t^{max}, \forall k \in \mathcal{H}_c \cup \mathcal{N}_{N_c}^{BH} \end{aligned}$$

- $R_{N_c}^{BH}$: *achieved data rate of IAB node* N_c *in the backhaul*
- P_{N_c}: *transmission power of IAB node* N_c *in the backhaul*
- P_{h_c}: *transmission power of access heliostat* $h_c, \forall h_c \in \mathcal{H}_c$
- $P_{N_{c'}}, \forall c' \in \mathcal{N}_{N_c}^{\mathcal{BH}}$: *transmission power of IAB node/IAB relay connected to the backhaul of IAB node* N_c

Energy efficiency optimization for IAB relays

- The optimization problem of the IAB nodes is formulated as follows.

$$\max_{P_{N_c}} EE_{N_c}\left(P_{N_c}\right) = \frac{R_{N_c}^{BH}}{\sum_{\forall c' \in \mathcal{N}_{N_c}^{\mathcal{BH}}} P_{N_{c'}} + P_{N_c}}$$

$$s.t.\ \boldsymbol{c1}:\ P_{N_c} \leq P^{max}$$

$$\boldsymbol{c2}:\ P_{N_{c+1}}^{S} \geq P^{S}$$

$$\boldsymbol{c3}:\ t_k^{E2E} \leq t^{max}, \forall k \in \mathcal{N}_{N_c}^{BH}$$

- $R_{N_c}^{BH}$: *achieved data rate of IAB node* N_c *in the backhaul*
- P_{N_c}: *transmission power of IAB node* N_c *in the backhaul*
- $P_{N_{c'}}, \forall c' \in \mathcal{N}_{N_c}^{\mathcal{BH}}$: *transmission power of IAB node/IAB relay connected to the backhaul of IAB node* N_c

Energy efficiency optimization for access heliostats

- The single-variable optimization problem of the access heliostats is formulated as follows:

$$\max_{P_{h_c}} EE_{h_c}(P_{h_c}, P_{-h_c}) = \frac{R_{h_c}^{AC}}{P_{h_c} + P_c}$$
$$\boldsymbol{c1}: P_{h_c} \leq P^{max}$$
$$\boldsymbol{c2}: P_{h_c,N_c}^{S} \geq P^{s}, \forall h_c \in \mathcal{H}_c$$
$$\boldsymbol{c3}:\ t_{h_c}^{E2E} \leq t^{max}, \forall h_c \in \mathcal{H}_c$$

- P_{h_c}: *transmission power of access heliostat* $h_c, \forall h_c \in \mathcal{H}_c$
- $R_{h_c}^{AC}$: *achieved data rate of heliostat* h_c *in the access.*

Latency

- The corresponding transmission delay experienced by heliostat h_c with the achieved data rate:

$$t_{h_c}^{E2E} = t_{h_c}^{AC} + t_{h_c}^{BH} + \sum_{\forall n \in \{N_{c+1}, \dots, |\mathcal{N}_{N_c}^{*}|\}} t_{N_n}^{BH} \leq t^{max}, \forall h_c \in \mathcal{H}_c$$

- Where, the delay experienced in the access network and the backhaul network of its own segment is given by $t_{h_c}^{AC} = \frac{D_{h_c}}{R_{h_c}^{AC}}$ and $t_{h_c}^{BH} = \frac{D_{N_c}}{R_{N_c}^{BH}}$, respectively.

- The rest of the term capture the latency experienced at the backhaul of the subsequent segment-heads within the route of data transmission from heliostat h_c to the CS.

Univ of New Mexico RFP 38488-002
Pathloss Model

- The <u>3GPP Pathloss Model</u> consists of two components, i.e., the Line of Sight (LoS) and the Non-Line of Sight (NLoS – due to the multi-path effect).
- The pathloss stemming from both LoS and NLoS events can be calculated by the closed-form equations (derived through real measurements in 3GPP).
- The probability of LoS and NLoS events, given the communication environment and distance can also be determined through the closed-form formula (similarly, through real measurements in 3GPP).
- The **pathlosses depend on** both the **2D distance** (Euclidean distance between x and y coordinates) **as well as 3D distance** (Euclidean distance among x, y, and z coordinates). Hence, as the heliostats move (elevation and/or azimuth angles change, the pathloss changes).

(x, y, z) | Elevation change (x’, y’, z) | Elevation + Azimuth change (x’, y’, z’)

Univ of New Mexico RFP 38488-002
Pathloss Model

- From the **3GPP pathloss model**, we consider the **Urban-Micro environment** which represents a busy wireless environment.
- The Urban-Micro environment only accounts for $d^{2D}_{h_c,h'_c} \geq 10m$. So, for $d^{2D}_{h_c,h'_c} < 10m$, the 3GPP pathloss model considers the wireless environment as an indoor office environment congested with wireless devices – closest possible to the CSP, where heliostats reside close to each other contributing high levels of interference.
- For different environments (Urban-Micro and office) the pathloss calculation varies. The equations are provided in the next slides.

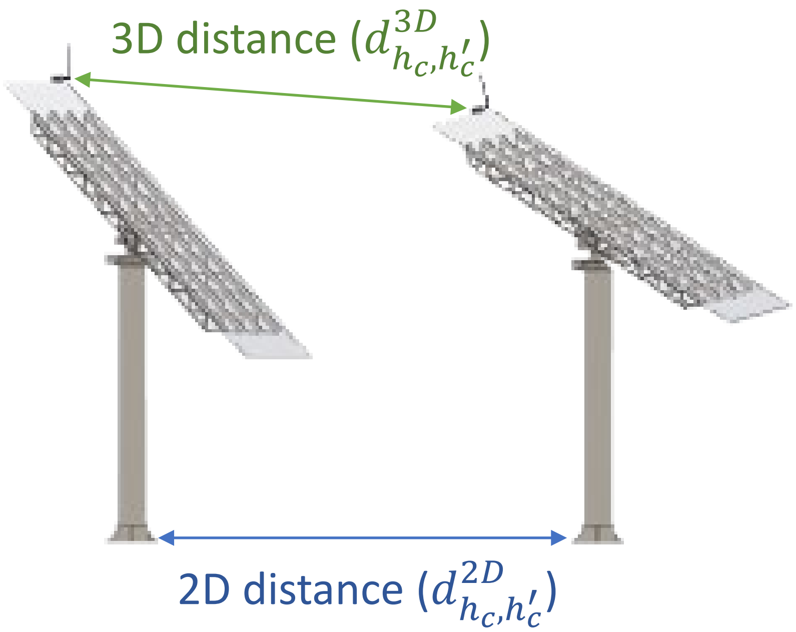

Univ of New Mexico RFP 38488-002
Pathloss Model

- The **LoS** pathloss:

$$PL^{LoS}_{h_c,h'_c} = \begin{cases} 32.4 + 17.3\log_{10}\left(d^{3D}_{h_c,h'_c}\right) + 20\log_{10}(f_c) \; ; d^{2D}_{h_c,h'_c} < 10 \; and \; 1m < d^{3D}_{h_c,h'_c} < 150m \\ 32.4 + 21\log_{10}\left(d^{3D}_{h_c,h'_c}\right) + 20\log_{10}(f_c) \; ; \; 10m < d^{2D}_{h_c,h'_c} < d_{BP} \\ 32.4 + 40\log_{10}\left(d^{3D}_{h_c,h'_c}\right) + 20\log_{10}(f_c) - 9.5\log_{10}\left(d^2_{BP} + \left(h_{h'_c} - h_{h_c}\right)^2\right) \; ; d_{BP} < d^{2D}_{h_c,h'_c} < 5km \end{cases}$$

- The **NLoS** pathloss:

$$PL^{NLoS}_{h_c,h'_c} = \begin{cases} max\left(PL^{LoS}_{h_c,h'_c}, 17.3 + 38.3\,log_{10}\left(d^{3D}_{h_c,h'_c}\right) + 24.9\,log_{10}(f_c)\right); d^{2D}_{h_c,h'_c} < 10 \; and \; 1m < d^{3D}_{h_c,h'_c} < 150m \\ max\left(PL^{LoS}_{h_c,h'_c}, 22.4 + 35.3\,log_{10}\left(d^{3D}_{h_c,h'_c}\right) + 21.3\,log_{10}(f_c) - 0.3\left(h_{h_c} - 1.5\right)\right); 10m \le d^{2D}_{h_c,h'_c} < 5km \end{cases}$$

where, f_c is the center frequency and d_{BP} is the breakpoint distance defined as $d_{BP} = \frac{4(h_{h_c}-h_E)\,(h_{h'_c}-h_E)f_c}{c}$, where $h_E = 1$ for Urban-Micro environment.

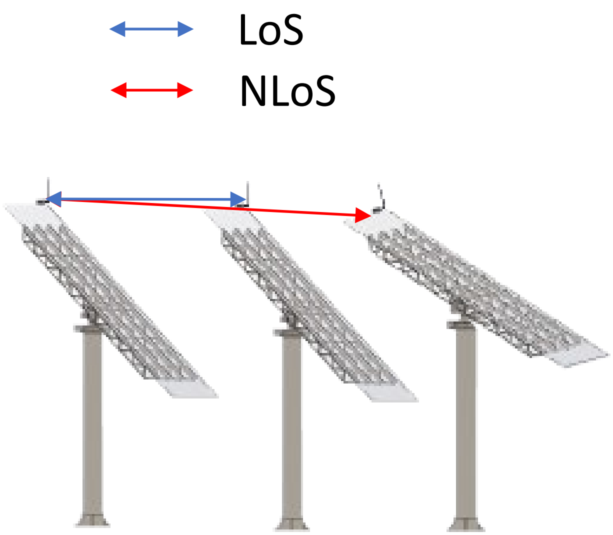

Univ of New Mexico RFP 38488-002
Pathloss Model

- The **probability of LoS pathloss** If $d^{2D}_{h_c,a_c}$<10m:

$$Pr^{LoS}_{h_c,h'_c} = \begin{cases} 1; \quad d^{2D}_{h_c,h'_c} \leq 1.2m \\ exp\left(-\frac{d^{2D}_{h_c,h'_c} - 1.2}{4.7}\right); \ 1.2m < d^{2D}_{h_c,h'_c} < 6.5m \\ exp\left(-\frac{d^{2D}_{h_c,h'_c} - 6.5}{32.6}\right); \ 6.5m < d^{2D}_{h_c,h'_c} \end{cases}$$

- Else:

$$Pr^{LoS}_{h_c,h'_c} = \begin{cases} 1; \quad 10m < d^{2D}_{h_c,h'_c} \leq \ 18m \\ \frac{18}{d^{2D}_{h_c,h'_c}} + exp\left(\frac{-d^{2D}_{h_c,h'_c}}{36}\right)\left(1 - \frac{18}{d^{2D}_{h_c,h'_c}}\right); \ 18m < d^{2D}_{h_c,h'_c} \end{cases}$$

- The resulting **overall pathloss**:

$$PL_{h_c,h'_c} = Pr^{LoS}_{h_c,h'_c} PL^{LoS}_{h_c,h'_c} + \left(1 - Pr^{LoS}_{h_c,h'_c}\right) PL^{NLoS}_{h_c,h'_c}$$

- The pathloss is used to define the communication channel gain as $g_{h_c,h'_c} = \frac{1}{10^{\frac{PL_{h_c,h'_c}}{10}}}$ that is used in the maximization of energy efficiency and minimization of the latency problems.

Univ of New Mexico RFP 38488-002
Position Updates

Elevation Angle (Side View)

Required parameters:

- Length of the mirror: L
- Height of mirror pivot: h
- Angle of elevation: $\angle e$ [degree]
- Height of the top of the mirror:

$$\sin(90^\circ - \angle e) = \frac{\boldsymbol{h'}}{L/2}$$

$$\Rightarrow \boldsymbol{h' = {}^{L}/_{2} \sin(90^\circ - \angle e)}$$

$$\therefore z' = h + \boldsymbol{h'}$$

- Updated position (x', y'):

$$x' = x$$

$$y' = y - \boldsymbol{{}^{L}/_{2} \sin(\angle e)}$$

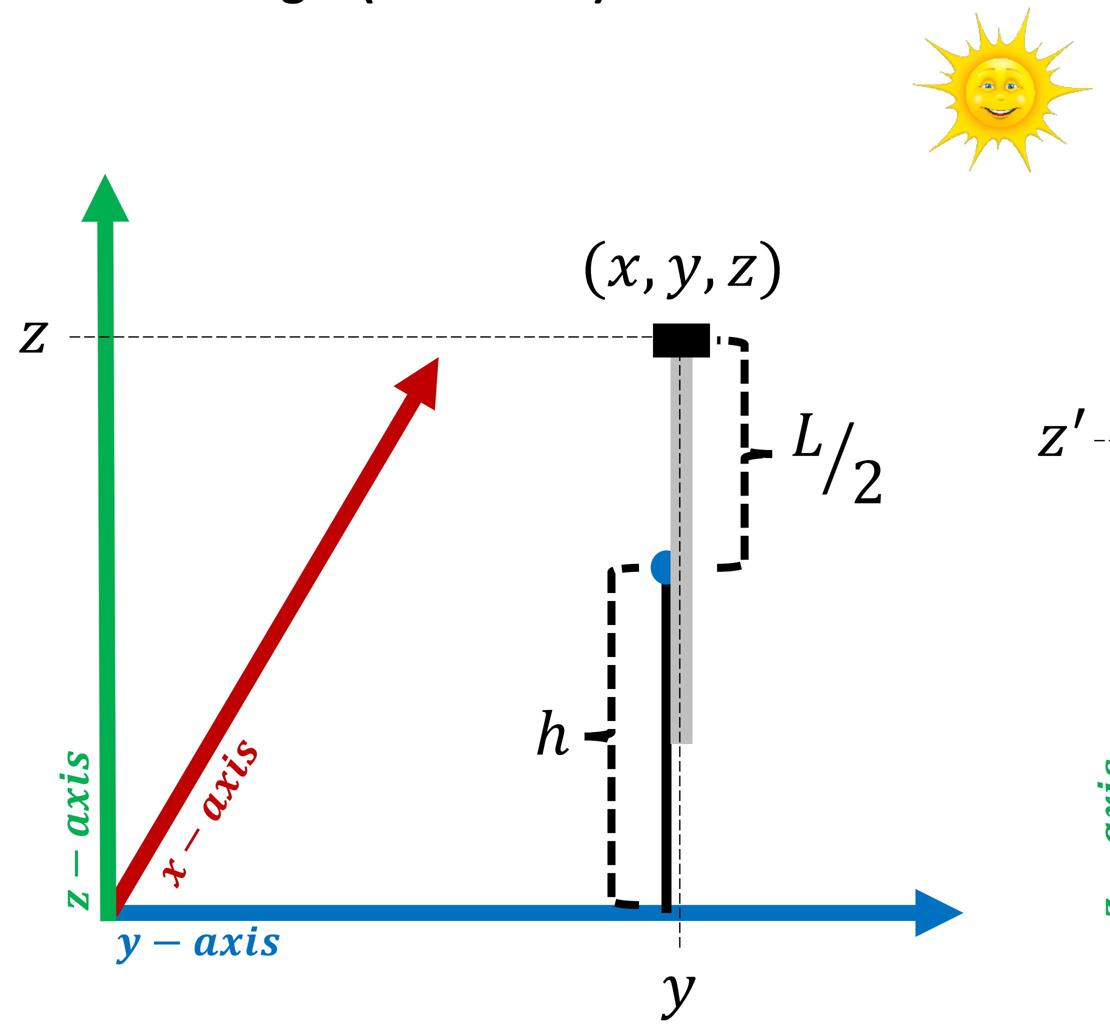

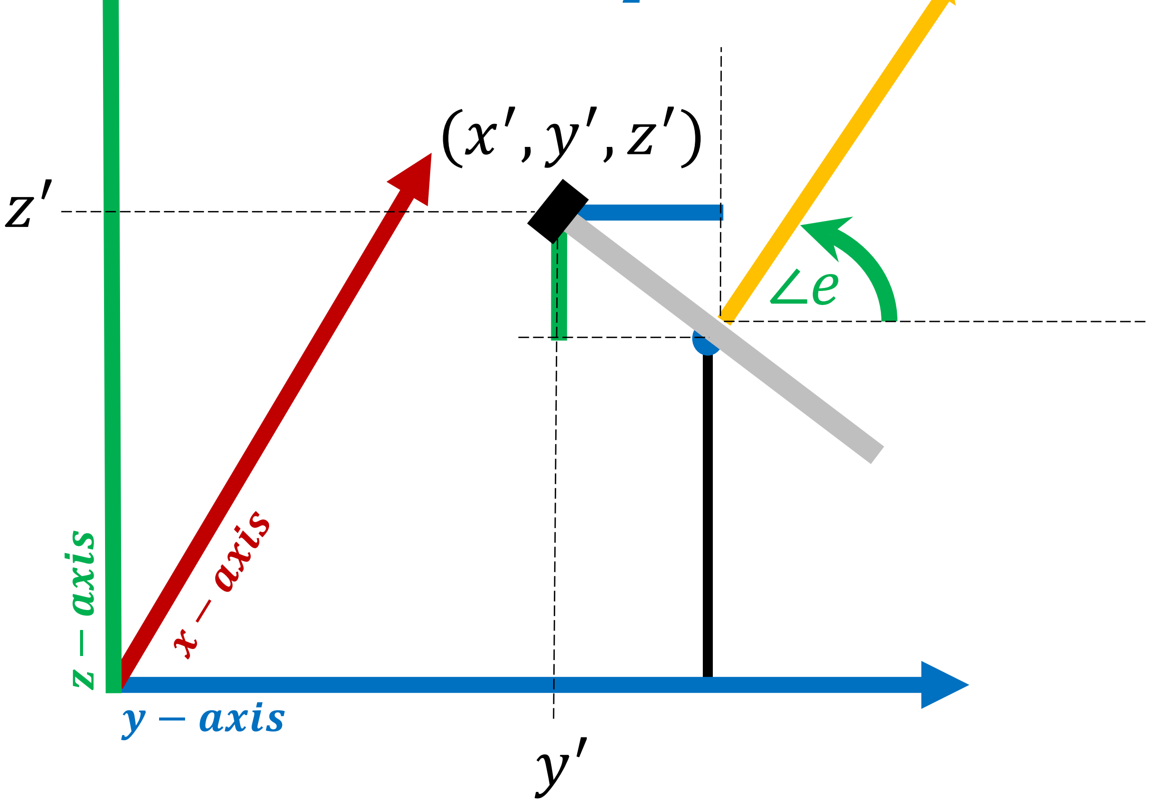

Univ of New Mexico RFP 38488-002
Position Updates

Required parameters:

- Length of the mirror: L
- Angle of azimuth: $\angle a$ [degree]
- Updated position (x', y', z'):

$$x' = x - \frac{L}{2}\sin(\angle a)$$
$$y' = y - \frac{L}{2}\cos(\angle a)$$
$$z' = z$$

Azimuth Angle (Top View)

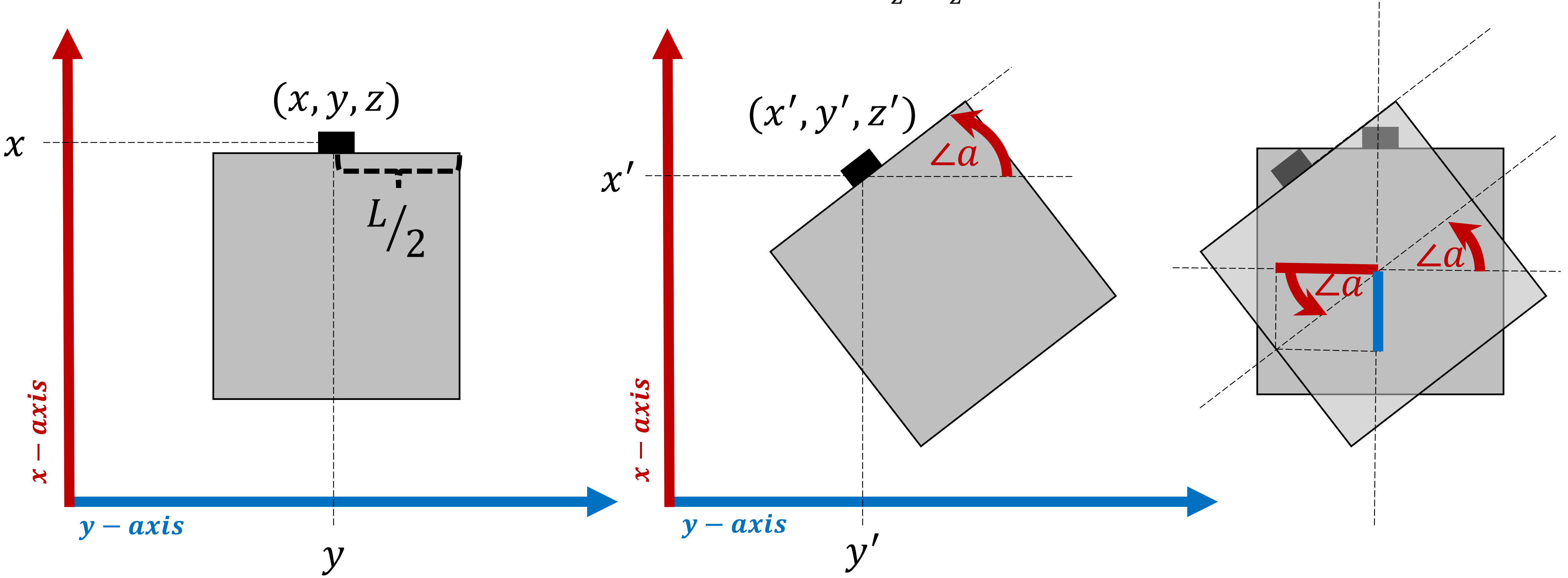

Univ of New Mexico RFP 38488-002
Simulation

- Completed the simulation for a 24-hour timeframe the max EE && min Latency optimization based on the energy and DNI data.
- In the 24-hour timeframe, the energy and DNI (Direct Normal Irradiance) data are taken as input after every 5 minutes to determine the mode of the heliostats.
- The heliostat can be in one of the two modes: “STANDBY” or “ACTIVE”.
  - **STANDBY** mode: Heliostats are not transmitting and only the “$\boldsymbol{energy_{standby}}$” in consumed.
  - **ACTIVE** mode: Heliostats are transmitting by consuming “$\boldsymbol{energy_{transmission}}$” and “$\boldsymbol{energy_{active}}$”.
- In ACTIVE mode and for a particular timestamp, heliostats are performing “NCLA” or both “CLA” and “NCLA” depending on the DNI in this timestamp.
- We have logged the battery status of each heliostat at every step of the simulation (at an interval of 5 minutes).
- The simulation was run on CARC (Center for Advanced Research Computing) at UNM with 32 cores and required 37.6 hours.

Simulation Parameters

$$\boldsymbol{time\_interval = 5 * 60\ [s]}$$

- $V_{DDS} = 3.6\ [V]$
- $I_{CORE}^{standby} = 2.92 * 10^{-6}\ [A]$
- $\boldsymbol{energy_{standby} = V_{DDS} * I_{CORE}^{standby} * time\_interval}$

- $V_{DDS} = 3.6\ [V]$
- $I_{CORE}^{active} = 2.89 * 10^{-3}\ [A]$
- $I_{PERIPHERAL} = 750.1 * 10^{-6}\ [A]$
- $V_{SENSOR} = 3.0\ [V]$
- $I_{SENSOR} = 808.5 * 10^{-6}\ [A]$
- $\boldsymbol{energy_{active} = \left(V_{DDS} * \left(I_{CORE}^{standby} + I_{PERIPHERAL}\right) + V_{SENSOR} * I_{SENSOR}\right) * time\_interval}$

- $\boldsymbol{battery_{max} = 324\ [KJ]\ \#\ 100\%}$
- $\boldsymbol{battery_{min} = 65\ [KJ]\ \#\ 20\%}$

Reference: TI CC1312R, Pages: 12, 62

Univ of New Mexico RFP 38488-002
Milestones and Tasks Progress

Simulation Parameters (continued)

- $Access\ Heliostats$:
  - $energy_{transmission} = P_{transmission} * t_h^{AC}\ [J]$
  - $t_h^{AC} = \frac{D_h}{R_h^{AC}}\ [s]$

- $Segment - head\ Heliostats$:
  - $energy_{transmission} = P_{transmission} * t_h^{BH}\ [J]$
  - $t_h^{BH} = \frac{D_{h+}\sum_{\forall h'} D_{h'}}{R_h^{BH}}\ [s]$

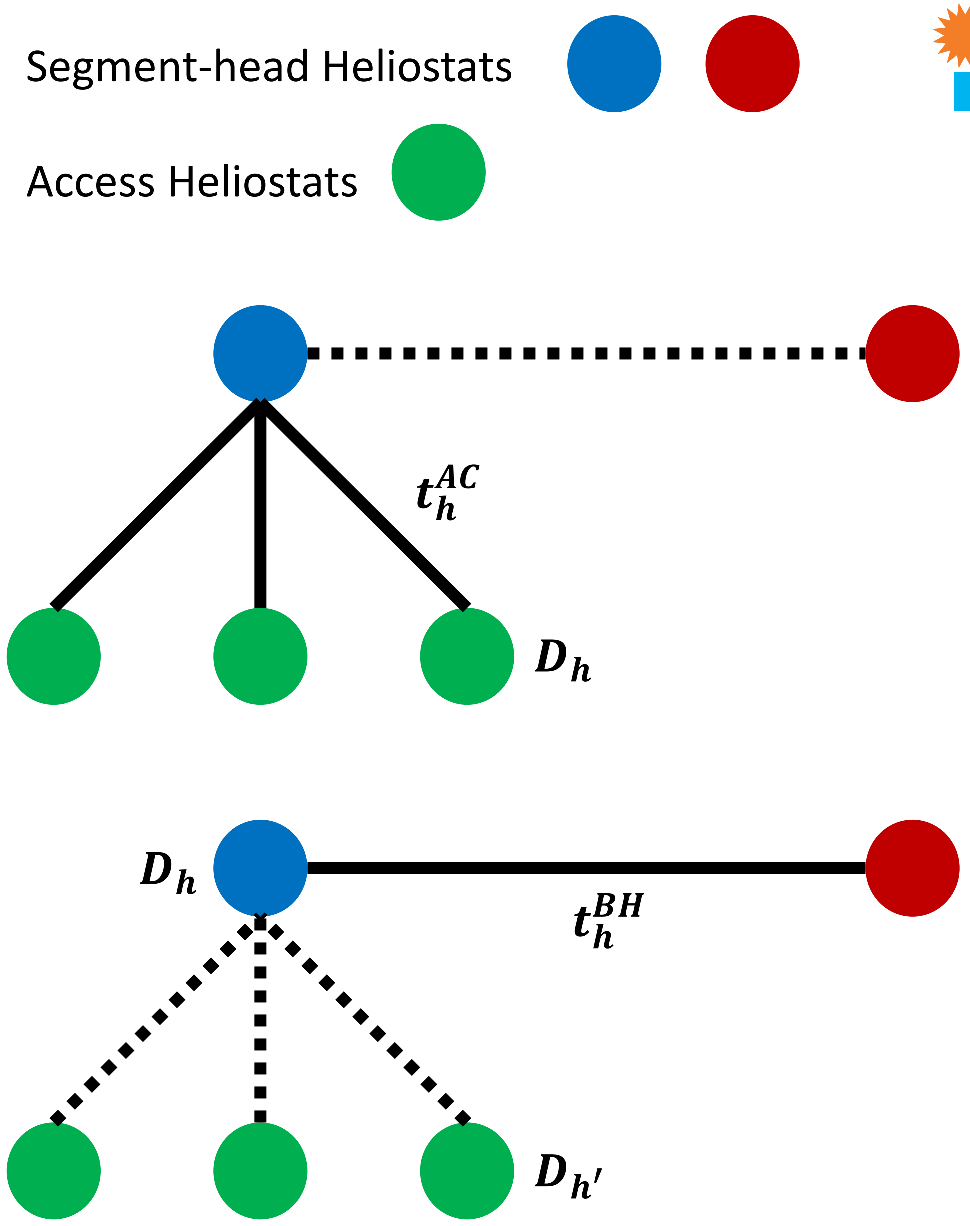

Simulation Overview

- timestamp after every 5 mins

  $\boldsymbol{energy_{harvested} = energy[timestamp]}$

  $\boldsymbol{energy_{consumed} = [0, \dots, 0]}$

- if DNI[timestamp] = 0

  mode = ‘STANDBY’, $\boldsymbol{energy_{consumed} \mathrel{+}= energy_{standby}}$

- else

  mode = ‘ACTIVE’

  - if DNI[timestamp] >= 500

    event = ‘CLA’, optimization_CLA(event)

    $\boldsymbol{energy_{consumed} \mathrel{+}= energy^{CLA}_{transmission} + energy_{active}}$

  event = ‘NCLA’, optimization_NCLA(event)

  $\boldsymbol{energy_{consumed} \mathrel{+}= energy^{NCLA}_{transmission} + energy_{active}}$

- $\boldsymbol{battery_{status} = battery_{status} + energy_{harvested} - energy_{consumed}}$

- The net energy is the difference between energy harvested and energy consumed.
- If there is positive net energy and the battery status is not $\boldsymbol{battery_{max}}$, the surplus energy harvested is added to the battery to have status set to $\boldsymbol{battery_{max}}$.
- If there is negative net energy, we subtract the net energy from the battery status.

Univ of New Mexico RFP 38488-002
Simulation Results

Battery Status

- We also performed battery status analysis for a day where 324KJ corresponds to 100% charge of battery.
- The consumption for the RF module to be active for transmissions and the consumption during the transmission is significantly smaller than the energy harvested.
- We also performed an **analysis for a week** where **energy harvest occurs only on Day 1** and **no harvest** occurs in the next consecutive **6 days**.
- Even in such worst-case, the charge of the battery did not drain enough to drive the heliostats RF module incapable of waking up.

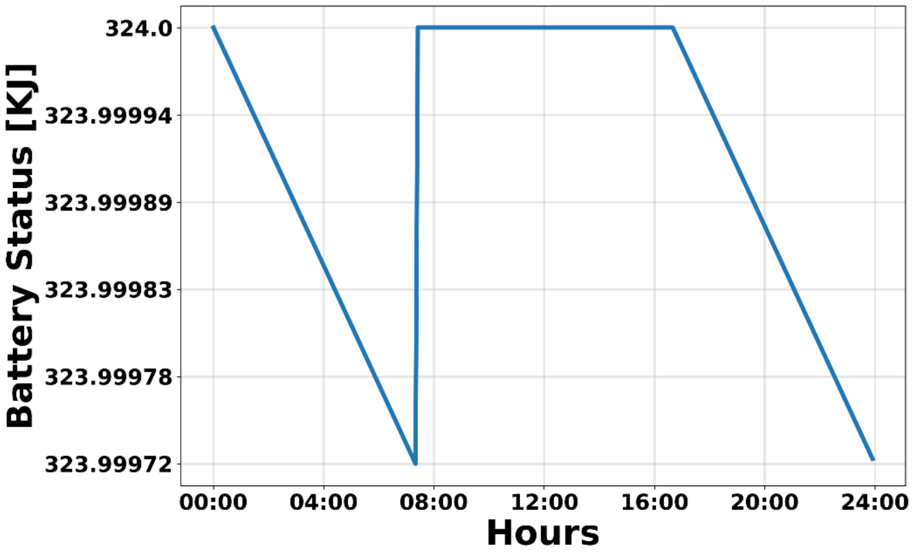

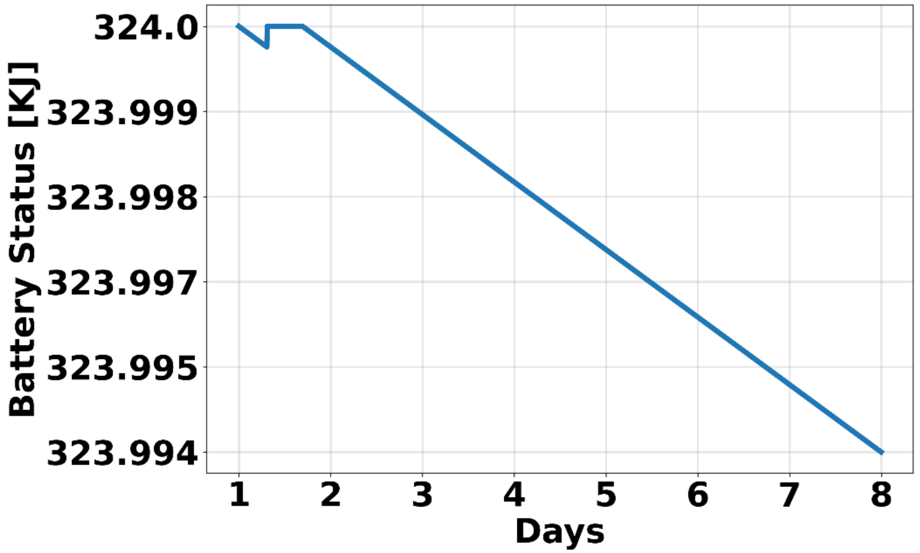

Univ of New Mexico RFP 38488-002
Simulation Results

Maximum Latency

- With the necessary data collected and having modified the problem of energy efficiency maximization and end-to-end latency minimization, we have simulated for a timeframe of 1 day (Jan 01, 2020).
- The day long simulation consisted of heliostats operating in standby modes (when the heliostats do not transmit or receive any data) and active modes (consisting of CLA and NCLA events).
- We have analyzed the achieved end-to-end latency in every possible CLA segment group performing CLA simultaneously and the corresponding NCLA segment group performing NCLA simultaneously.
- We have concluded to **not having any heliostats requiring an end-to-end latency more than the latency constraint**, both during CLA events and NCLA events, which have latency constraints of 250msec and 2sec, respectively.

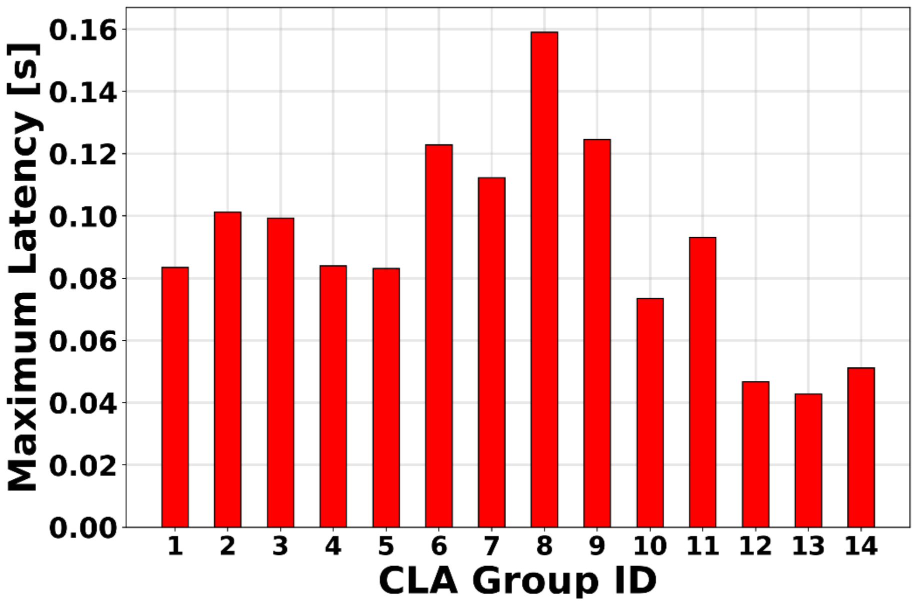

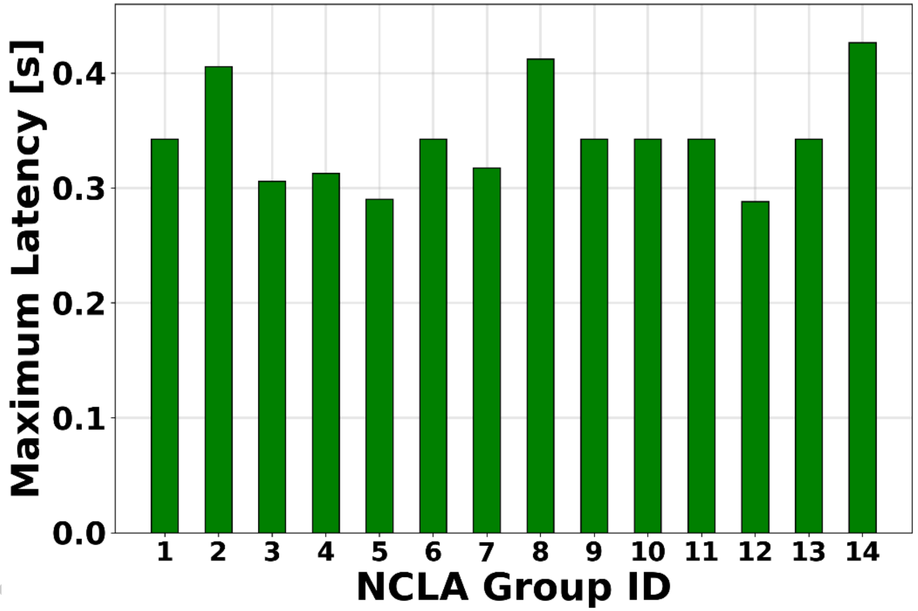

Univ of New Mexico RFP 38488-002
Emulation

- We have **built our own radio module** to consider our system model components including path loss, personalized transmission power, data rate, etc.
- We have **built our own UDP** (User Datagram Protocol) **Application for the IAB nodes** to collect packets from the access network and forward it to the next-hop destination.
- Scalability of wireless networks is limited in network emulators due to the broadcast nature of the communication.
- We are currently working on splitting the entire network into multiple emulation events and work on the log files to compile the results.

Backhaul Network

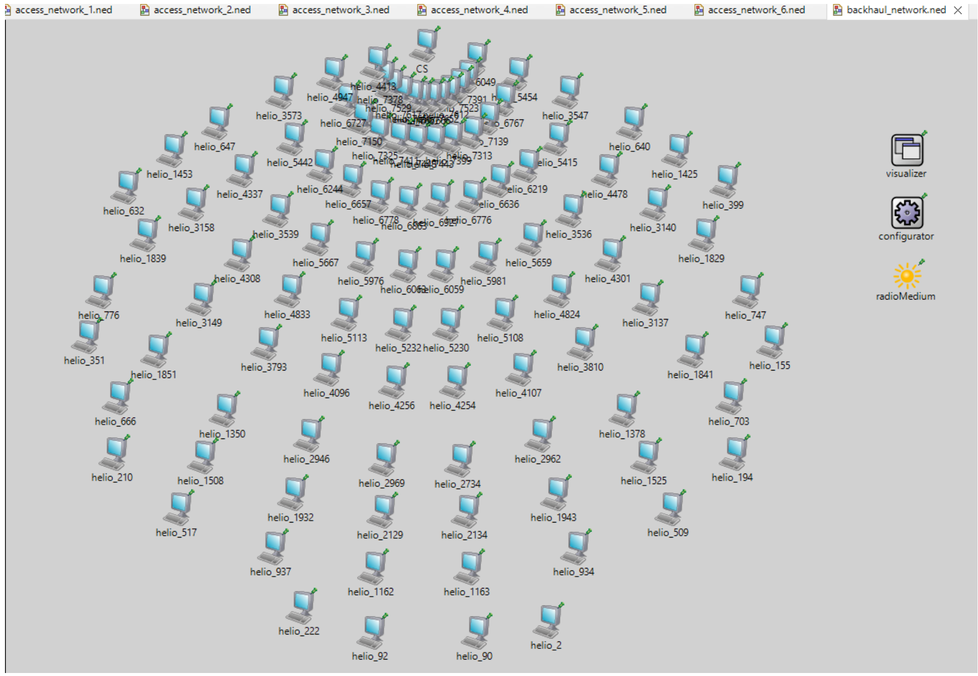

Access Networks

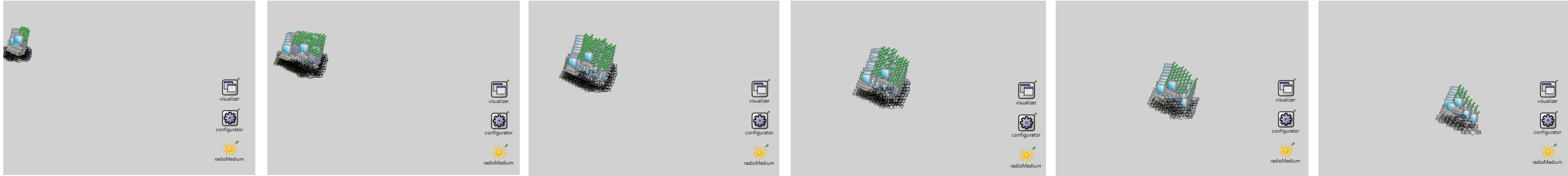

Univ of New Mexico RFP 38488-002
Next steps

- Testing of wireless communication protocols under the IAB-based network
- Dynamic clustering-based network reconfiguration
- Design an entropy-based routing
- Perform dynamic spectrum management in the access and wireless backhaul
- Implement intra- and inter-cluster interference mitigation
- Perform modeling and simulation
- Perform emulation-based experiments
- Partial HELIOCOMM validation at Sandia National Laboratories (SNL) National Solar Thermal Test Facility (NSTTF)

Thank you!

Eirini Eleni Tsiropoulou
Associate Professor
Computer Engineering Chair
Director of Recruiting and Admissions
Department of Electrical & Computer Engineering
University of New Mexico
eirini@unm.edu